CHAOS IN NON-EUCLIDEAN GEOMETRIES ARISING IN MECHANICS

by

Tapobrata Bhattacharya

A dissertation submitted to the faculty of
The University of North Carolina at Charlotte
in partial fulfillment of the requirements
for the degree of Doctor of Philosophy in
Mechanical Engineering

Charlotte

2015

Approved by:

____

Dr. Scott David Kelly

____

Dr. Russell Keanini

____

Dr. Christopher Vermillion

____

Dr. Mingxin Xu

____

Dr. Andrea Micheletti

ABSTRACT

TAPOBRATA BHATTACHARYA. Chaos in Non-Euclidean Geometries Arising in Mechanics. (Under the direction of DR. SCOTT DAVID KELLY)

Chaotic systems are a class of nonlinear dynamical systems that have captured the attention of mathematicians and engineers for long. Even though chaotic systems are deterministic in nature, long term prediction of behavior of such systems is difficult. Most of the studies on the evolution of such systems, have been restricted to the Euclidean manifold. The proposed dissertation will

1. Examine the dependence of elementary concepts from dynamical systems theory, particularly those that pertain to stability and measures of chaos, on the metric structure assigned to the space or manifold in which a dynamical system evolves.

2. Examine the way in which the input-output relationships defined by mechanical control systems with nonlinear dynamics, particularly systems representing problems in robotic locomotion, viewed as transformations between differentiable manifolds, affect measures of chaos.

The present research summarizes background material and preliminary results and explores chaos in the context of non-Euclidean manifolds. It also focuses on mechanical systems that have the ability to locomote by internal shape change. Such systems can be modeled by principal connections using geometric methods. The study involves investigating the flow of the differential equations that govern the motion of

the body under chaotic actuation of the shape parameters.

ACKNOWLEDGMENTS

I am indebted to my advisor Dr. Scott David Kelly for his infinite patience on me and for introducing me to the wonderful world of geometric mechanics. I am eternally grateful to Dr. Ronald Smelser without whose timely interventions this thesis would not have seen the light of the day. I shall remember with gratitude my colleagues, Rodrigo Abrajan Guerrero and Mike Fairchild for their assistance and participation in this research. I remember my family's great sacrifice for my education with deepest appreciation.

TABLE OF CONTENTS

LIST OF FIGURES

CHAPTER 1: THEORY OF MANIFOLDS AND EXTERIOR ALGEBRA

1.1 Introduction

A dynamical system is characterized by its configuration variables that completely identify the system. The set of all configuration variables is called the configuration space of the system. The configuration spaces are generally metric spaces, i.e., topological spaces that are equipped with a metric. As an example, the configuration spaces of dynamical systems that come up in this document are mostly Cartesian products of $SE(n)$, which are paracompact. A paracompact space is locally metrizable under certain conditions. In fact, every metric space satisfies the properties of paracompact spaces. Hence, the study of topological spaces provide a general framework to study convergence, continuity and compactness that lead up to the notion of special kinds of topological spaces, the manifolds. The following section illustrates some definitions and properties related to metric spaces. The proofs of the theorems can be found in [6].

1.2 Topological Spaces

Definition 1.2.1. (Topology) A topology τ on a set X is a collection of subsets of X, under the following conditions,

1. the empty set ϕ and X are open,

2. any arbitrary union of open sets remain open and

3. any finite intersection of open sets remain closed.

Definition 1.2.2. (Topological space) A topological space is an ordered pair (X, τ), such that the set X and τ (a topology on X) satisy the following,

1. the empty set ϕ and X are in τ,

2. any arbitrary union of open subsets of X is in τ and

3. any finite intersection of open subsets of X is in τ .

A topological space is a generalized notion of mathematical space. The differences in topological spaces arise on account of differences in the topologies assigned to the set. The notions of base for a topology and separation axioms are key to the definitions of manifolds. A base for a topology τ, where (X, τ) is a topological space, is a collection $\mathfrak{B}$, such that every open subset G of X can be expressed in terms of the indexed family $B_\alpha \in \mathfrak{B}$ as $G = \cup_\alpha B_\alpha$. If $\mathfrak{V}$ denotes the family of neighborhoods of $x \in X$, a neighborhood base for x is collection of neighborhoods $\mathfrak{B} \subset \mathfrak{V}$, such that $\forall V \in \mathfrak{V}$, $\exists B \in \mathfrak{B}$ satisfying $B \subset V$. A topological space X is first countable if it has a countable base for every $x \in X$. The set X is second countable if τ has a countable base. The separation axioms impose restrictions on topologies of spaces and are the basis of classification of topological spaces. The one space relevant to the theory of smooth manifolds is the Hausdorff space. A topological space X is Hausdorff or T_2, if for every pair of distinct points $x, y \in X$, there exists disjoint open sets that satisfy $x \in X$ and $y \in Y$. Hausdorff spaces are of significance as every sequence in a Hausdorff space converges to a unique limit point.

Definition 1.2.3. (Metric space) A metric space is a topological space (M, d), where M is a set with a metric d on itself. A metric is a function,

$$d\colon M \times M \to \mathbb{R}$$

such that the following holds for any $x, y, z \in M$:

1. $d(x, y) \geq 0$

2. $d(x, y) = 0 \iff x = y$

3. $d(x, y) = d(y, x)$ and

4. $d(x, z) \leq d(x, y) + d(y, z)$.

The metric spaces are characterized by the propeties of completeness, continuity and compactness.

1.2.1 Completeness

The definition of completeness of a metric space depends on the notion of convergence of a sequence. A sequence $\{x_n\}$ in X is convergent at $x \in X$ if for any $\epsilon > 0$, there exists $N(\epsilon) \in \mathbb{N}$, such that, $d(x_m, x) < \epsilon$ for all $m \geq N$. A sequence is a Cauchy sequence one for which any $\epsilon > 0$, there exists $N(\epsilon) \in \mathbb{N}$, such that, $d(x_m, x_n) < \epsilon$ for all $m, n \geq N$. The convergence of sequences is related to the idea of Cauchy convergence. Every convergent sequence is a Cauchy sequence. A metric space is complete if every Cauchy sequence converges to a point in X. A Banach space is a normed linear space that is complete with respect to the metric.

1.2.2 Continuity

The notion of continuity is fundamental in topology and can be defined in terms of mapping between open sets. Let (X, d_X) and (Y, d_Y) be metric spaces. A function $f\colon X \to Y$ is continuous at $x \in X$, iff for any $\epsilon > 0$, there exists $\delta(\epsilon) > 0$ such that if $d_X(x, y) < \delta(\epsilon)$, then $d_Y(f(x), f(y)) < \epsilon$ where $y \in X$. Function continuity in metric spaces is generally defined in terms of sequences. If there exists a sequence $\{x_n\}$ in X such that $x_n \to x$ for $f(x_n) \to f(x)$, then the map $f\colon X \to Y$ is continuous at $x \in X$. A continuous function is a function that is continuous at all points in the metric space.

1.2.3 Compactness

The extension of a property that is defined at a point, to the entire space, depends on the set being compact. The property of compactness ensures the retention of properties of finite sets. An open cover of a set S is a family of indexed subsets $\{U_\alpha\}_{\alpha \in A}$ that contain the set S for all U_αs being open sets. A metric space is said to be compact if each of its open cover has a finite subcover, *i.e.*, there exists a finite subset J of A satisfying $X \subset \cup_{\beta \in J} U_b eta$. Alternatively, convergence of sequences is used to define compact sets on metric spaces. A metric space X is compact if every sequence in X has a converging sequence in X. This notion of compactness is known as sequential compactness. An important result with regard to compact subsets of $\mathbb{R}^n$ is the Heine-Borel theorem.

Definition 1.2.4. (Heine-Borel theorem) The following statements are equivalent for a subset S of the Euclidean space $\mathbb{R}^n$,

1. S is closed and bounded,

2. S is compact and

3. every open cover of S has a finite subcover (or every sequence in S has a convergent subsequence).

1.3 Manifold

The theory of manifolds with added algebra for differentiability is central to the analysis of physical systems. The systems dealt with in the succeeding chapters are systems whose configuration spaces are Lie groups. The dynamics of such systems can be expressed in terms of reduced configuration variables by exploiting symmetry. The definitions, theorems and lemmas are gleaned from [12] , [16] and [22].

Definition 1.3.1. (Manifold) An n dimensional topological space M is a manifold if it satisfies the following criteria,

1. M is Hausdorff (i.e. any two points in M are separated by discrete neighbourhood),

2. M is second countable (i.e. there exists a local countable basis for M) and

3. for any arbitrary point in M, there exists an open open neighborhood that is homeomorphic to a subset of $\mathbb{R}^n$.

A coordinate chart on an n-manifold M is a pair (U, ϕ). For any point $p \in M$, there exists a neighborhood $U \subset M$ and a homeomorphism $\phi \colon U \to \mathbb{R}^n$. The vector $\phi(q) = \{q^1, ..., q^n\}$ are local coordinates on M when $q \in U$. The number of basis vectors of a coordinate chart of an open subset on an n-dimensional manifold is n. A collection of coordinate charts $S = \{(U_\alpha, \phi_\alpha)\}_{\alpha\in I}$ is called an atlas of M, if M can be written as a union of coordinate charts, $\{U_\alpha\}_{\alpha\in I}$. α is an element of an indexed array set I. The functions $f_{\alpha\beta}$ and $f_{\beta\alpha}$, known as transition maps, are homeomorphisms defining the change of coordinates between two coordinate charts. All topological manifolds are constructed by global union of coordinate charts that are related to each other by homeomorphism. If the change of coordinate maps happen to be diffeomorphisms, then the manifold is differentiable or smooth. The rich structure of differentiable manifolds enable one to do calculus on manifolds.

Definition 1.3.2. If $S = \{(U_\alpha, \phi_\alpha)\}_{\alpha\in I}$ be the atlas of a topological manifold M, such that the transition maps $f_{\beta\alpha} = \phi_\beta \circ \phi_\alpha^{-1}$ are k-times continuously differentiable, then S is known as a C^k atlas. A C^k atlas determines a C^k structure on the manifold and M is called a C^k differentiable manifold.

Definition 1.3.3. Two overlapping coordinate charts (U_α, ϕ_α) and (U_β, ϕ_β) are said to be compatible if

1. $\phi_\alpha(U_\alpha \cap U_\beta)$ and $\phi_\beta(U_\alpha \cap U_\beta)$ are open subsets of $\mathbb{R}^n$,

2. $f_{\beta\alpha} = \phi_\beta \circ \phi_\alpha^{-1} \colon \phi_\alpha(U_\alpha \cap U_\beta) \to \phi_\beta(U_\alpha \cap U_\beta)$ and

   $f_{\alpha\beta} = \phi_\alpha \circ \phi_\beta^{-1} \colon \phi_\beta(U_\alpha \cap U_\beta) \to \phi_\alpha(U_\alpha \cap U_\beta)$ are infinitely differentiable.

A smooth atlas has compatible coordinate charts for every pair. An atlas, $S = \{U_\alpha, \phi\}_{\alpha\in I}$ of M is called a C^∞ atlas, if all composition maps of the nature $\phi_\beta \circ \phi_\alpha^{-1}$ are C^∞ maps. A manifold is smooth or differentiable if it has a smooth atlas. A C^∞ manifold is a manifold with a C^∞ structure.

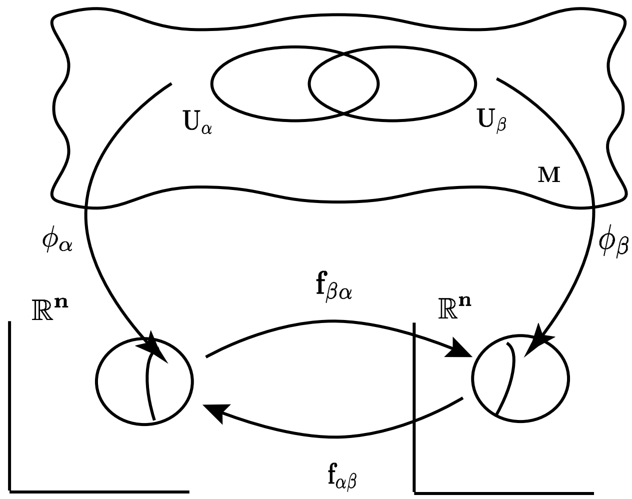

Figure 1: Compatible coordinate charts

1.3.1 Submanifold

Any open subset of a C^∞ manifold is equipped with the structure of a C^∞ manifold. A submanifold can be viewed as images of level sets arising out of either immersion or submersion or embedding. A smooth map $f\colon M \to N$ is an immersion if the derivative Df is an injection; in other words, rank of the derivative of the linear map is equal to the dimension of M. An immersed submanifold is the image of an immersion map. It is worthwhile to note that the immersion map need not be injective to be a submanifold. The map f is a submersion, if Df is a surjection. The rank of the derivative of the map is equal to the the dimension of N. An embedding is a special kind of immersion. It is homeomorphic to its image under the map $f(M) \subset N$ (topological embedding). The map f determines the subspace topology that the embedded submanifold inherits. All immersions do not necessarily give rise to embeddings. An injective immersion $f\colon M \to N$ that satisfies,

1. f is closed

2. f is proper and

3. M is compact

is an embedding.

Definition 1.3.4. (Embedded submanifold) An embedded submanifold of M is a subset $S \subset M$ with the property that for each $q \in S$, there exists an open neighborhood U and a set of coordinate functions $q_1, ..., q_k$, such that $S \cap U = \{q \in S \colon q_{k+1} = ... = q_n = 0\}$.

The dimension of the submanifold is given by k, a positive integer. Any open subset of M is a locally closed submanifold. It means that every point $q \in S$ admits an open neighborhood U of q in a manner that $U \cap S$ is closed in U [19]. For a smooth map between two manifolds, $f \colon M \to N$, the set of regular values is the set of points in the open neighborhood of $f^{-1}(c)$ in M, where $T_q f$ is surjective; $q \in M$ and $f(q) = c$. Then c is called the regular point.

1.3.2 Tangent vectors, tangent spaces and vector fields

A curve $\gamma(t)$ on a manifold is a one parameter map $t \mapsto M$ for any parameterization t. Two curves on a manifold $\gamma_1(t)$ and $\gamma_2(t)$ are equivalent at a point $q \in M$ if

(i) $\gamma_1(0) = \gamma_2(0) = p$ and

(ii) $(\phi \circ \gamma_1)'(0) = (\phi \circ \gamma_2)'(0)$

for some coordinate chart (U, ϕ).

Definition 1.3.5. A tangent vector at q is the equivalence class of curves passing through q.

Alternatively, if $\gamma(t)$ is any curve on M and $\gamma(0) = q$, the tangent vector at q is given as,

$$v_q = \frac{d(\gamma(t))}{dt}\,|_{t=0}; \forall t \in \mathbb{R} \tag{1.3.1}$$

If the coordinates on a n-dimensional manifold at point are designated as $\{x_1, .., x_n\}$ then the standard basis for tangent vectors at the point is given by $\frac{\partial}{\partial x^1}, ..., \frac{\partial}{\partial x^n}$. Tangent vectors on a manifold can also be defined in terms directional derivatives.

Definition 1.3.6. For any scalar function f defined on M, the tangent vector at q is the map $f \mapsto D_{v_q} f$ known as the directional derivative of f at q.

It can be written as,

$$D_{v_q}(f(q)) = \frac{df}{dt} f(q + tv)|_{t=0} = (f \circ \gamma(t))'(0) \tag{1.3.2}$$

The tangent space at $q \in M$, denoted by $T_p M$, is the linear vector space of all tangent vectors at q. A tangent bundle of a manifold M is the disjoint union of all tangent spaces to M, denoted as,

$$TM = \cup_{q \in M} T_q M \tag{1.3.3}$$

For an n-dimensional manifold, the dimensions of the tangent space and tangent bundle are n and $2n$ respectively.

Definition 1.3.7. (Derivative of a map) Let $f \colon M \to N$ be a smooth map. The derivative of f, at point $q \in M$, is defined as,

$$T_q f(\dot{\gamma(0)}) = \frac{d}{dt}(f \circ \gamma)|_{t=0} \tag{1.3.4}$$

for a curve $\gamma(t)$ in M such that, $\gamma(0) = q$ and $\dot{\gamma(0)} = v_q$.

The notation of the derivative of the map or tangent map of f varies from $f_*(q)$ to $Df(q)$. If π_M and π_N denote the bundle projection maps, then the following diagram commutes.

$$\begin{array}{ccc} TM & \xrightarrow{Tf} & TN \\ {\scriptstyle \pi_M}\downarrow & & \downarrow{\scriptstyle \pi_N} \\ M & \xrightarrow[f]{} & N \end{array}$$

In local coordinates, the Jacobian of the map f evaluated at q represents the linear tangent lifted map.

Definition 1.3.8. (Vector field) A vector field X on a manifold M is a map $X\colon M \to TM$ that assigns a tangent vector $X(q) \in T_qM$ to every point $q \in M$.

If π_M denotes the projection map on to the first coordinate, $\pi_M\colon TM \to M$, then a smooth vector field is a smooth section of TM and $\pi_M \circ X = Id_M$.

$$\begin{array}{c} TM \\ {\scriptstyle \pi_M}\downarrow \\ M \end{array}$$

A smooth vector field is a differentiable map from M to TM. The real vector space of vector fields on M is denoted as $\mathfrak{X}(M)$.

Definition 1.3.9. An integral curve of X is a map $\gamma(t)\colon t \to M$, with initial condition $\gamma(0)$ at $t = 0$, such that $\dot{\gamma} = X(\gamma(t)), \forall t \in (a, b)$, (a, b) being an open interval in $\mathbb{R}$.

The flow of a vector field X on M is a collection of maps $\phi_t \colon M \to M$ such that $t \to \phi_t(\gamma(0))$ is the integral curve of X with initial condition $\gamma(0)$. If ϕ_t be the flow of a smooth vector field X on a manifold M, then

- ϕ_0 is the identity map (i.e. $\phi_0(p) = p, \forall p \in M$),
- $\phi_{t+s} = \phi_t \circ \phi_s$ and
- the map $\phi_t \colon M \to M$ is diffeomorphic.

Definition 1.3.10. A 1-form on a manifold M at point p is an assignment of a linear operator or a covector that maps a tangent vector at T_pM to $\mathbb{R}$.

The cotangent space at $p \in M$ is the vector space of all such linear functionals (covectors) and is denoted by T_p^*M; the cotangent space being dual to the tangent space T_pM. The disjoint union of all cotangent spaces on M is the cotangent bundle. It may be noted that both the tangent and the cotangent bundle have the natural structure of a vector bundle on the manifold. Just as tangent vectors provide a coordinate-free definition of derivative of a curve in a manifold, the derivative of a real valued function or differential on a manifold are the cotangent vectors.

1.4 Exterior Algebra

Exterior algebra on manifolds, also called wedge product or Grassmann algebra, is an algebraic construction to study areas, volumes and other higher dimensional constructs. The study of exterior algebra is also called *Ausdehnungslehre* or extension calculus. The material for this section is sourced from [9], [19].

1.4.1 Differential forms — revisited

A general expression of a k-form β on a manifold M is of the construction

$$\beta(q) = \sum_{1 \leq i_1, \ldots, i_2 \leq n} F_{i_1, \ldots, i_k}(q) dx_{i_1} \wedge dx_{i_2} \wedge \ldots dx_{i_k} \tag{1.4.1}$$

for $q \in M$. A function on M is a 0-valued form. The map β is an element of the vector space designated by $T_q^* M$, dual to the vector space $T_q M$. The multiplication in the algebra of differential forms is called the *wedge product* and is used to generate higher dimensional forms. In general, β on M is an assignment of a skew-symmetric k-fold multilinear map,

$$\beta(q) = T_q M \times \ldots \times T_q M \rightarrow V \tag{1.4.2}$$

at each point q. The skew-symmetric property ensures that

$$\beta(q)(V_1, \ldots, V_i, V_j, \ldots V_k) = -\beta(q)(V_1, \ldots, V_j, V_i, \ldots V_k) \tag{1.4.3}$$

for $V_i \in T_q M$. If α is a k-form and β is a l-form, then the wedge product of the two forms is a $(k + l)$-form.

$$(\alpha \wedge \beta)(q) = \frac{(k + l)!}{k! l!} A(\alpha \otimes \beta) \tag{1.4.4}$$

for $q \in M$. A is the alteration operator that acts on a $(0, p)$ tensor t by

$$A(t)(V_1, \ldots, V_p) = \frac{1}{p!} \sum_{\pi \in S_p} sgn(\pi) t(V_{\pi(1)}, \ldots, (V_{\pi(p)}) \tag{1.4.5}$$

where $sgn(\pi)$ is the sign of permutation π,

$$sgn(\pi) = \begin{cases} +1 & \text{if } \pi \text{ is even;} \\ \\ -1 & \text{if } \pi \text{ is odd;} \end{cases} \tag{1.4.6}$$

and S_p is the permutaion group of the set $1, 2, ..., p$. The operator A skew-symmetrizes the p-multilinear maps [19].

1.4.2 Exterior algebra — continued

Definition 1.4.1. (Exterior product) If $f: M \to V$ be a smooth function (0-form) on a smooth manifold M, the extrior derivative of f, also known as the differential is a smooth linear map $df: TM \to V$.

In general, a the exterior derivative of a k-form is a $(k+1)$-form. A differential k-form is closed if $d\alpha = 0$ and is said to be exact if it can be expressed as $\alpha = d\beta$ for any $(\beta - 1)$-form. Every exact form is closed. The exterior product of a general k-form $\beta(q) = \sum_{1 \leq i_1, ..., i_2 \leq n} F_{i_1,...,i_k}(q) dx_{i_1} \wedge dx_{i_2} \wedge ...dx_{i_k}$ is computed as

$$d\beta = \sum_{1 \leq i_1, ..., i_2 \leq n} dF_{i_1,...,i_k}(q) \wedge dx_{i_1} \wedge dx_{i_2} \wedge ...dx_{i_k} \tag{1.4.7}$$

where $dF_{i_1,...,i_k}(q)$ is evaluated in the same manner as differential of a 0-form.

Definition 1.4.2. (Interior product) If X be a vector field and β be a k-form on M, then the interior product of X with α is a $(k-1)$-form defined as,

$$X \lrcorner \alpha(q)(V_2, ..., V_k) = \beta(q)(X, V_2, ..., V_k) \tag{1.4.8}$$

for $q \in M$.

Proposition 1.4.3. The differential of a smooth function $f: M \to \mathbb{R}$ is the 1-form df such that, for any $p \in M$, $df(p)\colon T_pM \to \mathbb{R}$ is the differential or derivative of f at p.

Relative to a choice of local coordinates the basis for T_p^*M, dual to the basis $\frac{\partial}{\partial x^i}$ for T_pM, is denoted by dx^i. The differentilal for a smooth function $f\colon M \to \mathbb{R}$ is given by,

$$df(p) = \frac{\partial f}{\partial x^i} dx^i \tag{1.4.9}$$

.

1.4.3 Lie derivative, pullback and push-forward of forms

Analogous to the fact that a smooth map between manifolds induces a linear map on the tangent vectors, a dual map, the pullback, exists on the cotangent vectors.

Definition 1.4.4. (Pullback) If $f\colon M \to N$ is a diffeomorphism between manifolds, from M to N and $v_1, ..., v_k \in T_P M$ for any $p \in M$, then the pullback of a k-form, α on N, is defined as

$$(f^*\alpha)(p)(v_1, ..., v_k) = \alpha(f(p))(T_pf.v_1, .., T_pf.v_k). \tag{1.4.10}$$

The push-forward for any diffeomorphism $f\colon M \to N$ is defined by $f_* = (f^{-1})^*$. The pullback and push-forward commute with $\wedge$ and d operations. The pullback of a function g defined on a manifold N, by a diffeomorphism $f\colon M \to N$ is the function f^*g on M, given by,

$$f^*g = g \circ f. \tag{1.4.11}$$

The push-forward of a function h defined on a manifold M, by a diffeomorphism

$f\colon M \to N$ is the function f_*h on N, given by,

$$f_*h = h \circ f^{-1}. \tag{1.4.12}$$

The pullback of a vector field Y on a manifold N, by a diffeomorphism $f\colon M \to N$ is the vector field f^*Y on M, given by,

$$f^*Y = (f^{-1})_*Y = Tf^{-1} \circ Y \circ f. \tag{1.4.13}$$

Likewise, the push-forward of a vector field X on manifold X, by a diffeomorphism $f\colon M \to N$ is the vector field f_*X on N, given by,

$$f_*X = Tf \circ X \circ f^{-1}. \tag{1.4.14}$$

The Lie derivative of a vector field or a differential form provides a natural choice of formulation of derivative along a vector field or the flow of a vector field. Let $\phi_t\colon M \to M$ be the flow of a vctor field X on M. At any $q \in M$,

$$X_q = \frac{d}{dt}\phi_t|_{t=0}. \tag{1.4.15}$$

Definition 1.4.5. (Lie derivative of vector fields) The Lie derivative of a vector field Y in M, along the flow ϕ_t of a vector field X, is the vector field

$$\mathcal{L}_X Y(q) = \lim_{t \to 0} \frac{1}{t}[Y_q - (\phi_{t*}Y)_q]. \tag{1.4.16}$$

The push-forward of the vector field Y by the flow map is defined by, $T_{\phi_{-t}(q)}Y_{\phi_{-t}(q)}$. It may be noted that ϕ_t is locally diffeomorphic, i.e., $\phi_t^{-1} = \phi_{-t}$.

Definition 1.4.6. (Lie derivative of differential forms) The Lie derivative of a differential form α, along the flow ϕ_t of a vector field X, is defined as

$$\mathcal{L}_X\alpha(q) = \lim_{t\to 0}\frac{1}{t}[(\phi_t^*\alpha)(q) - \alpha(q)]. \tag{1.4.17}$$

The pullback of the form by the flow $\phi_t^*\alpha$ is defined by, evaluating α at p and pushing forward the tangent vectors by the derivative of the flow map.

Theorem 1.4.7. (Lie derivative theorem) The Lie derivative theorem states that

$$\frac{d}{dt}\phi_t^*\alpha = \phi_t^*\mathcal{L}_X\alpha. \tag{1.4.18}$$

Cartan's magic formula provides a means of computing Lie derivative of k-form α, along a vector field X on a manifold M.

$$\mathcal{L}_X\alpha = d(X\lrcorner\alpha) + X\lrcorner d\alpha. \tag{1.4.19}$$

If $g\colon M \to \mathbb{R}$ is a function on a manifold M; X be a vector field on M, then the Lie derivative of g along X is given by the directional derivative of g along X.

$$\mathcal{L}_X\alpha(q) := X[f](q) = df(q)\cdot X. \tag{1.4.20}$$

for $q \in M$. If ϕ_t is the flow associated with the vector field X; $\phi_0 = q$ and $\cdot\phi_0 = X(q)$; the formula can be rewritten as

$$\mathcal{L}_X\alpha := \frac{d}{dt}|_{t=0} f\circ\phi_t(q). \tag{1.4.21}$$

Definition 1.4.8. (Jacobi-Lie bracket) If X and Y are two vector fields on a manifold M, then, the Jacobi-Lie bracket of X and Y is a unique vector field $[X, Y]$ on M.

If $g\colon M \to \mathbb{R}$ is a derivation(function) on M, the Jacobi-Lie bracket is given by the equation

$$[X, Y][g] = X[Y[g]] - Y[X[g]]. \tag{1.4.22}$$

The Lie derivative of the vector field Y along X may be defined as $\mathcal{L}_X Y = [X, Y]$. For finite dimensional manifolds, the formula for Jacobi-Lie bracket assumes the form,

$$[X, Y]^j = X^i \frac{\partial Y^j}{\partial x^i} - Y^i \frac{\partial X^j}{\partial x^i} = (X \cdot \nabla)Y^j - (Y \cdot \nabla)X^j. \tag{1.4.23}$$

It can be shown that that Lie derivative of a vector field Y along a vector field X, $\mathcal{L}_X Y$, is equal to the Jocobi-Lie bracket of X and Y, $[X, Y]$.

1.4.4 Orientable manifold

Let M be an $n-$dimensional manifold with $u_1, ..., u_n$ and $v_1, ..., v_n$ being two ordered bases for the tangent space T_pM at $p \in M$. If the determinant of the derivative of the linear transformation between the two bases is positive,then the two bases are said to be equivalent. In case of manifolds, orientation is decided by the choice of tangent space orientation. An orientation of M at p is defined to be the equivalence class of all ordered bases of the linear vector space T_pM. If p be any point $p \in M$ and the orientation of M remains the same irrespective of choice of p, then M is orientable at p. M is said to be an oriented manifold. Mobius strips and Klein bottles are examples of surfaces that are not orientabled in a global sense. The exterior algebra provides an elegant expression of classical Stokes theorem in terms of exterior derivative of differential forms.

Theorem 1.4.9. (Stokes theorem) Let M be a compact, oriented, n-dimensional manifold with an (n-1)-form β on M. If ∂M denotes the boundary on M, then

$$\int_{\partial M} d\beta = \int_M \beta. \tag{1.4.24}$$

1.5 Riemannian Manifold

The notion of a Riemannian manifold is essential to the study of non-Euclidean manifolds. As one of the goals of the thesis is to study chaotic systems in the context of non-Euclidean setting, a brief outline of the theory of Riemannian manifolds is presented here [15]. Riemannian manifolds fall under the category of complete and normed spaces, the Banach spaces. A Riemannian manifold is a manifold that is equipped with a smoothly varying inner product, defined on the tangent space at each point in the manifold. An inner product induces a norm, which in turn induces a metric. A Riemannian metric g is a 2-tensor field on the manifold M, that is bilinear, symmetric and positive-definite. The inner product $g(q)$ defined on T_qM for each $q \in M$ is smooth, meaning that the components of the metric tensor g_{ij} are smooth functions of coordinates q. The formula for inner product is expressed as $< v_q, w_q >_q = g(q)(v_q, w_q) = g_{ij} v_q^i w_q^j$; $v_q, w_q \in T_qM$. The two vectors are said to be orthogonal to each other if $< v_q, w_q >_q = 0$. The corresponding norm is given in local coordinates as $< v_q, v_q >_q = g(q)(v_q, v_q) = g_{ij} v_q^i v_q^j$. Every manifold can be given a Riemnannian metric; this can be proved by using the partition of unity. Let (M_1, g_1) and (M_2, g_2) be two Riemannian manifolds. A diffeomorphism ϕ: $M_1 \to M_2$ is an isometry, if $\phi^* g_2 = g_1$ (alternatively, $T^*\phi(g_2) = g_1$). The (M_1, g_1) and (M_2, g_2) belong to the same equivalence class if they are isometric to each other. The composition and inverses of isometries are isometries themselves. The group of isometries of a Riemannian manifold is an isometry group. The isometry group is a finite dimensional Lie group that acts smoothly on M [12].

The evolution of the Lorenz equations are analyzed on the $\mathbb{S}^2$ and the hyperbolic model, which are Riemannian manifolds. The Lorenz vector fields are also studied as image of local connection form for mechanical systems that can be modeled as principal fiber bundle. The theory of Riemannian manifolds play a key role in setting up of the problem in both cases.

CHAPTER 2: DYNAMICAL SYSTEMS AND CHAOS

2.1 Autonomous Dynamical Systems

A smooth, continous-time and autonomous dynamical system, on a smooth manifold Ω, can be modeled by the ordinary differential equation,

$$\dot{x}(t) = f(x) \tag{2.1.1}$$

where $x \in \Omega$ and $t \in \mathbb{R}$. The vector field $f(x)$ is a C^∞ map from $\mathbb{R} \times \Omega \to T\Omega$. The phase space of the dynamical system is denoted by Ω which is an open subset of $\mathbb{R}^n$. The integral curves of the vector field $f(x)$ corresponding to various initial conditions, constitute flows of the vector field in the phase space. A flow ϕ_t can be viewed as a map $\phi_t \colon \Omega \to \Omega$ where,

$$\dot{\phi}_t(x) = f(\phi_t(x)), \tag{2.1.2}$$

$\forall x \in \Omega$ and $t \in \mathbb{R}$. The definition of some of the terms that have been used extensively in the upcoming treatment of the subject, is enunciated hereafter [32],[27]. All subsequent theory is relevant for continuous time dynamical systems.

2.1.1 Orbits

The flow of a vector field is associated with orbits through points in phase space.

Definition 2.1.1. (Orbit) An orbit of a dynamical system γ_x, for a point $x \in \Omega$, is the set given by,

$$\gamma_x = \{\phi_t(x) | t \in \mathbb{R}\}. \tag{2.1.3}$$

A *semipositive* orbit through x is the set

$$\gamma_x^+ = \{\phi_t(x) | t \geq 0\}. \tag{2.1.4}$$

A *seminegative* orbit through x is the set

$$\gamma_x^- = \{\phi_t(x) | t \leq 0\}. \tag{2.1.5}$$

2.1.2 Invariant set

Definition 2.1.2. (Invariant set) A set $M \subseteq \Omega$ is invariant with respect to the flow map ϕ_t, if for any point $x \in M$ and any $t \in \mathbb{R}$, $\phi_t(x) \in M$.

In other words, all complete orbits through all points in M remain within M. M is a positively invariant set if $\phi_t(M) \subseteq M$ for all time $t \geq 0$. M is negatively invariant if $\phi_t(M) \subseteq M$ for all time $t \leq 0$.

Definition 2.1.3. (Invariant manifold) An invariant set $M \subseteq \Omega$ is an invariant manifold if it has the differentiable structure of a $C^r(r \geq 1)$ smooth manifold.

A positively or negatively invariant set is positively or negatively invariant, respectively, if it possesses the smooth structure of a $C^r(r \geq 1)$ differentiable manifold.

2.1.3 Limit set

The long term behavior of a dynamical system is characterized by its limit set. It is the state of the system after passage of infinite time, either going forward or backward in time.

Definition 2.1.4. (Limit set) The ω-limit point x_0 of any $x \in \Omega$, denoted by $\omega(x)$, is the limiting point of a sequence $\{t_i\}$, $t_i \to \infty$, such that,

$$\lim_{i \to \infty} \phi_{t_i}(x) = x_0 \tag{2.1.6}$$

if such limit exists.

An α-limit point is defined in terms of limit of the sequence for $\{t_i\} \to -\infty$.

An ω-limit set $\Omega(x)$ is the set of all ω-limit points of x. The basin of attraction B_Ω of an attracting ω-limit set Ω, is the union of all open neighborhoods U of $\Omega(x)$ such that $\Omega(x) = \Omega$ for all $x \in U$. The set of all intial conditions that evolve towards Ω, as $t \to \infty$, constitute the basin of attraction. The types of limit sets are of the following kind:

1. Fixed points: a fixed point is a point $x \in \mathbb{R}^n$, for which $\phi_t(x) = x; \forall t$.

2. Periodic orbits: a periodic orbit is characterized by $\phi_t(x) = \phi_{t+T}(x)$, where $T > 0$ is called the time period of flow. A limit cycle is a periodic, closed orbit that is the limit set of some other trajectory.

3. Quasiperiodic orbits: If there are more than one frequency in the periodic solution of the system the trajectories are given by the solution $\phi_t = H(\omega_1 t, ..., \omega_n t)$. The function H is periodic on $\omega_1 t, ..., \omega_n t$s with period being 2π. The frequency vector ω, given by $(\omega_1 t, ..., \omega_n t)$, is called the basis frequency vector. A solution with $n-$frequency base with frequencies being irrational multiples is diffeomorphic to the T^n torus. A T^n torus is the Cartesian product of $S^1 \times ... \times S^1$, where each S^1 represents a base frequency.

4. Strange attractors: The presence of strange attractors is indicative of chaotic dynamics. The steady state trajectories of such systems are bounded and display sensitive dependence to initial conditions. A small perturbation in initial conditions causes exponential divergence of trajectories in the long term. The trajectories converge to strange attractors that have fractal geometry, meaning that strange attractors have complex Hausdorff dimensions. A list of Hausdorff dimensions for fractals sets can be had in reference Falconer [5].

2.1.4 Nonlinear systems: Local stability

The local behavior of a nonlinear dynamical system can be examined qualitatively by studying the behavior of a linearized system. The Hartman-Grobman theorem states that the nonlinear system has the same qualitative behavior as that of a linear system about a hyperbolic fixed point [26].

Theorem 2.1.5. (Hartman-Grobman theorem) Let Ω be an open subset of $\mathbb{R}^n$, $f \in C^1(\Omega)$ and ϕ_t be the flow of an autonomous nonlinear system $\dot{x} = f(x)$. If $\dot{x}(0) = 0$ and the matrix $A = Df(x_0)$ has eigenvalues that have nonzero real parts (x_0 is hyperbolic), then there exists a homeomorphism $h\colon U \to V$, where U and V are open sets that contain the origin, such that on an open interval $I_0 \subset \mathbb{R}$, containing the zero for each $x_0 \in U$, for all x_0 and $t \in I_0$, h maps orbits in of the nonlinear system onto orbits of the linearized system in a manner that preserves time parameterization; i.e.,

$$h \circ \phi_t(x_0) = e^{At} h(x_0). \tag{2.1.7}$$

2.1.5 Chaos in dynamical systems

Chaotic systems fall under the category of a special class of nonlinear dynamical systems. A typical chaotic system is not stochastic and exhibits unpredictability with small change in initial conditions. Chaos in dynamical systems has been the object of much research; since Edward Lorenz chanced upon chaos in a dynamical system in the 1960s while creating a mathematical model for weather patterns. The term 'butterfly effect' is oft used to describe the essence of chaos and it signifies the sensitivity of a chaotic dynamical system to initial conditions. Chaos in deterministic dynamical systems is characterized by

1. topological transitivity or mixing,
2. closely packed aperiodic orbits and
3. sensitivity to initial conditions.

There is no universal definition of chaos. According to Devaney, for a metric space X, a discrete map $f\colon X \to X$ is chaotic if,

1. f is transitive,
2. the periodic points in f are dense in X and
3. f is sensitive to initial conditions.

A map f is transitive, if for any two nonempty subsets U and V in the phase space, there exists a natural number n such that, $f^n(U) \cap V$ is nonempty [4]. The second condition implies that periodic points of f form a dense subset in X. A map f is sensitively dependent on intial conditions if for any real $\epsilon > 0$ and any $x \in X$, there exist a natural number n and a y in the neighborhood of x, for which the $n-th$ iteration maps $f^n(x)$ and $f^n(y)$ are at a distance more that ϵ apart. However, if condition 1 and 2 are satisfied then the map f is sensitive to initial conditions [1].

2.1.6 Lyapunov exponents

The separation of trajectories in the phase space of the system is characterized by Lyapunov exponents. They measure the extent to which two integral curves diverge, starting from nearby intial conditions. A chaotic system has at least one positive Lyapunov exponent. A system with positive Lyapunov exponent evolves in a manner that makes prediction impossible beyond a period of time, that is characteristic of the system. The Lyapunov exponent is also a measure of the time scale on which the system dynamics becomes unpredictable. Several approaches have been put forth for numerically computing Lyapunov exponents by Bennetin et.al. [2] and Wolfe et.al.[33].

Given an n-dimensional continuous-time dynamical system, an initial n-sphere of initial conditions of infinitesimal δx-radius gets deformed to an n-ellipsoid under deformations of the phase space. The magnitude of the local stretching or contraction of the phase space is of exponential order. The trajectories of the locally linearized system are of exponential order of the eigenvalues. In general, for an n-dimensional system, there are n Lyapunov exponents; the largest and the smallest Lyapunov exponents correspond to the directions of maximum and minimum deformations of the phase space.

For computation of Lyapunov exponents, consider two initial conditions, x_0 and $x_0 + \delta x(0)$ in the phase space, separated by infinitesimal distance $\delta x(0)$ apart. If the flow corresponding to the vector field defining the evolution of the system be ϕ_t then, after time t the initial points get mapped to $\phi_t(x_0)$ and $\phi_t(x_0 + \delta x(0))$ respectively. The separation at time t is

$$\delta x(t) = \phi_t(x_0 + \delta x(0)) - \phi_t(x_0). \tag{2.1.8}$$

Linearizing the first term of the right hand side about x_0 one gets,

$$\delta x(t) = \phi_t(x_0 + \delta x(0)) - \phi_t(x_0) = D_{x_0}\phi_t(x_0).\delta x(0) \tag{2.1.9}$$

The Lyapunov exponent, that is the average exponential rate of stretching or contraction of the phase space can be written as,

$$\lambda(x(0), \delta x(0)) = \lim_{t\to\infty} \frac{1}{t} \frac{||\delta x(t)||}{||\delta x(0)||} = \lim_{t\to\infty} \frac{1}{t} ||D_{x_0}\phi_t(x_0).\delta x(0)||, \tag{2.1.10}$$

where $||\delta x(t)||$ is the standard Euclidean vector norm derived from inner product.

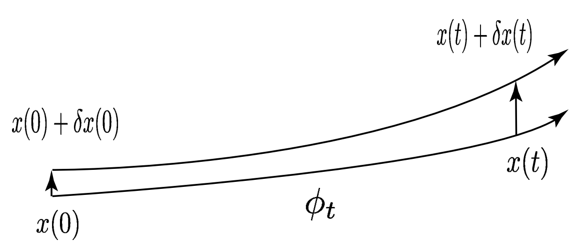

Figure 2: Separation of trajectories

According to Oseledec's ergodic theorem, the limit on the right hand side of the eqution exists under certain weak smoothness conditions and is finite and is equal to the Lyapunov exponent over the entire phase space [24].

2.1.7 Computation of Lyapunov exponents

There exist different numerical schemes for computing the Lyapunov exponents of a smooth continuous-time dynamical system. In this research, three numerical schemes have been implemented for the purpose of computing the Lyapunov exponents.

1. Largest Lyapunov exponent using distance metric: The largest Lyapunov exponent is computed by measuring the separation of trajectories and evaluating the logarithmic rate of separation. The method calls for rescaling of the separation distance after each iteration. The number of iterations necessary for convergence is dependent on the characteristic of the system and choice of initial condition.

2. Lyapunov spectrum by method of Jacobian: For any continuous-time dynamical system of the form (1), with initial condition x_0 chosen to lie on the attractor on the limit set, the Lyapunov exponents of the system can be calculated using (2). A ball of initial conditions of radius δx around an intial condition x_0, under the flow map $\phi_t(x_0)$, gets mapped from $x_0 + \delta x$ to $x(t) + J\delta x$; where the Jacobian J of the flow map ϕ_t is evaluated at x_0. From geometric standpoint, a sphere of initial conditions gets mapped to an ellipsoid by the Jacobian map. An initial set of tangent vectors q_0 evolves according to the following equation,

$$\dot{q}(t) = D_x f(x_0).q_0,\ q_0 = I. \tag{2.1.11}$$

[25]. The expression $D_x f(x_0)$ is the spatial derivative of the flow $\phi_t(x_0)$ evaluated at x_0. A system of coupled differential equations is then solved for $x(t)$

and $q(t)$ with initial conditions x_0 and q_0. The coupled equations assume the form,

$$\dot{x}(t) = f(x, t)$$
$$\dot{q}(t) = D_x f(x_0).q_0 \tag{2.1.12}$$

with initial conditions $x(0) = x_0$ and $(0) = q_0 = I$, the identity matrix. The above mentioned variational equation is solved for a time step T, whereby x_0 maps to x_T and q_0 to q_T. The Gram-Schmidt orthonormalization procedure is applied to q_T to yield a new basis v_T that spans the same subspace as spanned by q_T. The Lyapunov exponents for n iterations are computed by the equation,

$$\lambda_i = \lim_{n\to\infty} \frac{1}{nT} \sum_{i=1}^{N} \log ||v_T^i||. \tag{2.1.13}$$

3. Lyapunov spectrum for time series data: The method of computing the Lyapunov spectrum from chaotic time series data involves computing the linearized flow map of the tangent space by approximation of the Jacobian of flow [28]. If $\{x_j\} = x(t_0 + (j-1)\Delta\tau)$ be a discrete data set, where $j = (1, 2, 3, ...)$, the displacement vectors y_i of a set of datapoints $\{x_{k_i}\}$, for $k = \{1, 2, 3, ...\}$, that lie inside an ϵ-ball about x_j, is given as

$$\{y_i\} = \{x_{k_i} - x_j | ||x_{k_i} - x_j|| \leq \epsilon\}. \tag{2.1.14}$$

After evolution of the system by a single time step $T = n\Delta t$, for some integer n, the data points x_{k_i} and x_j get mapped to $x_{k_{i+n}}$ and x_{j+n} respectively. For infinitesimally small ϵ the tangent vector approximation y_i is mapped to

$$z_i = A_j y_i \tag{2.1.15}$$

The matrix A represents the linearized flow map of the system, i.e. the linear transformation of the tangent vectors between tangent spaces at x_j and x_{j+n}. A is computed by employing the least-square-error evaluation alogrithm that minimizes the average of the squared error norm of z_i and $A_j y_i$. The components of the A matrix for a n-dimensional system is given by the following set of equations:

$$V_{kl} = \frac{1}{n}\sum_{i=1}^{n} y_{ik} y_{il}, \tag{2.1.16a}$$

$$C_{kl} = \frac{1}{n}\sum_{i=1}^{n} z_{ik} y_{il}, \tag{2.1.16b}$$

$$A_j V = C. \tag{2.1.16c}$$

The term y_{ik} and z_{il} denote the k-th and l-th terms of the tangent vectors y_i and z_i respectively. The evolution of an initial set of basis for the tangent space e_j is computed by the map $A_j e_j$. The mapped basis $A_j e_j$ is orthonormalized using Gram-Schmidt orthonormalization technique in order to ensure orthogonality of the basis vectors. The Lyapunov exponents can be computed by the expression,

$$\lambda_i = \lim_{n\to\infty} \frac{1}{nT} \sum_{i=1}^{n} \log ||A_j e_j||. \tag{2.1.17}$$

The Jacobian matrix in general, is not diagonal or diagonizable or constant. But by polar decomposition theorem, the matrix J can be decomposed into the product of a rotation tensor R and a stretch tensor U,

$$J = RU. \tag{2.1.18}$$

The matrix R is an orthogonal matrix with determinant +1 and U is symmetric positive definite matrix. The positive real eigenvalues $\lambda_1, ..., \lambda_n$ for an n-dimensional system, of matrix U are called *principal stretches*. The eigenvectors of U, given by $u_1, ..., u_n$ are orthogonal and indicate the directions of the principal stretches at the x_0 and are known as *principal axes of strain*. In case of the map from a sphere of initial conditions to an ellipsoid, the principal stretch directions correspond to the semi-axes of the ellipsoid. The stretching is positive for $\lambda_i > 1$ and negative or compressive for $\lambda_i < 1$. In continuum mechanics parlance U is the *left Cauchy-Green strain tensor*,

$$J^T J = U \tag{2.1.19}$$

The same formulation can be arrived at by considering the *right Cauchy-Green strain tensor* V, written as,

$$J = VR \tag{2.1.20}$$

V and U are connected by the relation $V = RUR^T$. The eigenvectors $v_1, ..., v_n$ correspond to the principal stretch directions at $x(t)$ after having flown along the flow ϕ_t from initial condition $x(0)$.

The finite-time Lyapunov exponents can be approximated as

$$\lambda(x_0, t) = \lim_{t\to\infty} \frac{1}{t} \frac{||\delta x(t)||}{||\delta x(0)||} = \lim_{t\to\infty} \frac{1}{t} \frac{||J\delta x(0)||}{||\delta x(0)||} = \lim_{t\to\infty} \frac{1}{2t} (\hat{e} J^T J \hat{e}) \tag{2.1.21}$$

where $\hat{e} = \frac{\delta x(0)}{||\delta x(0)||}$. The equation (2.1.21) ensures that the Lyapunov exponents depend only on the initial orientation and not on the vector $\delta x(0)$.

2.1.8 Lorenz System

The Lorenz system is a set of differential equations that was developed by Edward Lorenz in 1963 as a mathematical model for earth's atmospheric convection. It is a simplification of the governing equations for two-dimensional flow problem. The Lorenz equations are,

$$\dot{x} = \sigma(y - x), \tag{2.1.22a}$$

$$\dot{y} = x(\rho - z) - y, \tag{2.1.22b}$$

$$\dot{z} = xy - \beta z. \tag{2.1.22c}$$

The solutions to the equations are chaotic for $\sigma = 10$, $\beta = \frac{8}{3}$ and $\rho = 28$. In addition, the inital conditions must lie on the attractor or on the basin of attraction. for the system to exhibit chaotic behavior. The coefficients σ and β are sometimes called the *Prandtl number* and *Rayleigh number* respectively. The plot of the chaotic solution of the Lorenz system is termed as gives rise to the strange attractor.

The Lorenz attractor is an example of chaos in a deterministic system. The system has one globally stable equilibrium, the origin, for $\rho < 1$. A supercritical bifurcation occurs at $\rho = 1$; giving rise to two additional symmetric pair of attracting fixed points at $(\sqrt(\beta(\rho - 1)), -\sqrt(\beta(\rho - 1)), \rho - 1)$. The new equilibrium points are stable, if, $\rho < \sigma\frac{\sigma+\beta+3}{\sigma-\beta-1}$.

The strange attractor is characterized by complex fractal geometry. Their Hausdorff dimension lies between $2.05 - 2.07$ and the correlation dimension is estimated to be $2.04 - 2.06$ [31].

CHAPTER 3: FILTERING CHAOS

An appropriate approach to model the dynamics of a rigid body in a fluid is to introduce the added mass or virtual mass effect. A body undergoing acceleration or deceleration in a fluid medium, displaces the surrounding fluid. The displaced fluid has the effect of increasing the inertia of the body; the added inertia term being the added mass of the system. An outline on the theory of added mass can be found in [14], [21]. A non axisymmetric planar body will experience non uniform distribution of added mass. Consequently, an ellipse moving in a plane in an ideal fluid, will have less translational inertia along the direction of the major axis, as compared to translational inertia along the minor axis. A case in point could be an ellipse in the configuration space SE(2), acted upon by an external force, in a manner such that the momentum vector field is chaotic and is measured with respect to body fixed coordinates. The inertia of the body effectively scales the momentum vector field along the direction of major axis, minor axis and rotation axis. In this dissertation the effect of inertia on the dynamics of body in presence of chaotic actuation of of the momentum vector field is studied. The nature of flows of the vector field, over a range of variation of inertia values is investigated. The chaotic forcing of the ellipse is implemented by applying the Lorenz vector field as externally applied momentum vector field, in the body fixed frame. The second integral of motion yields the evolution of the body and is examined for existence of strange attractors. The present research explores the case where the momentum vector field is actuated chaotically. The objective is to determine whether the input differential equations remains chaotic or not, after scaling by inertia terms. The system can be construed as a filter that resizes the chaotic vector fields that pass through it. The vector field studied in the present case is the Lorenz equations.

3.1 Lorenz Equations

The Lorenz system is a set of third order nonlinear ordinary differential equations. The equations are attributed to the mathematician Edward Lorenz who formulated the equations as a simple model for atmospheric convection. The Lorenz system is one of the earliest instances of a *strange attractor*. A detailed study of the equations can be found in [30], [31]. The set of equations are

$$\dot{x} = \sigma(y - x) \tag{3.1.1a}$$

$$\dot{y} = x(r - z) - y \tag{3.1.1b}$$

$$\dot{z} = xy - bz \tag{3.1.1c}$$

where σ, b and r are parameters characteristic to the system. The Lorenz system has been studied in detail over its dependency of the r parameter. The salient features of the Lorenz equations are,

1. the system has symmetry (invariant under the transformation $S(x, y, z) = S(-x, -y, -z)$),

2. the system is dissipitive in nature, i.e. the divergence of the vector field is negative and

3. there is a trapping region for which orbits of all points that lie on the interior to the region, stay inside the region.

One can define a Lyapunov function and show that there exists an ellipsoidal trapping region, where all solutions of Lorenz equations lie. The system parameters for the Lorenz equations are typically set at $\sigma = 10, b = \frac{8}{3}$. As r is varied over a range of values, the system exhibits interesting dynamics.

1. The origin is globally stable for $0 < r < 1$. At $r = 1$, the origin loses its stability, giving rise to two stable equilibrium ponts, C^+ and C^-. This event is a pitchfork bifurcation.

2. C^+ and C^- lose their stability at a critical value of $r = r_H$ and Hopf bifurcation occurs. The value of r_H turns out to be $r_H = \frac{\sigma(\sigma+b+3)}{\sigma-b-1}$, provided $\sigma - b - 1 > 0$. The fixed points are marked by presence of unstable limit cycles as the Hopf bifurcation is *subcritical*.

3. The strange attractor appears for $r = 28$ (Fig.3).

4. A series of infinite period doubling bifurcations take place, as r is tuned up from 0.99524 to 100.795.

3.2 Lyapunov Exponents Of Strange Attractor

Lyapunov exponents are a local measure of divergence of nearby trajectories - a singular feature of any chaotic system. The number of Lyapunov exponents of the Lorenz system is three, as the dimension of the system is three. The set of Lyapunov exponents of a system is called a spectrum. There is an abundance of literature on

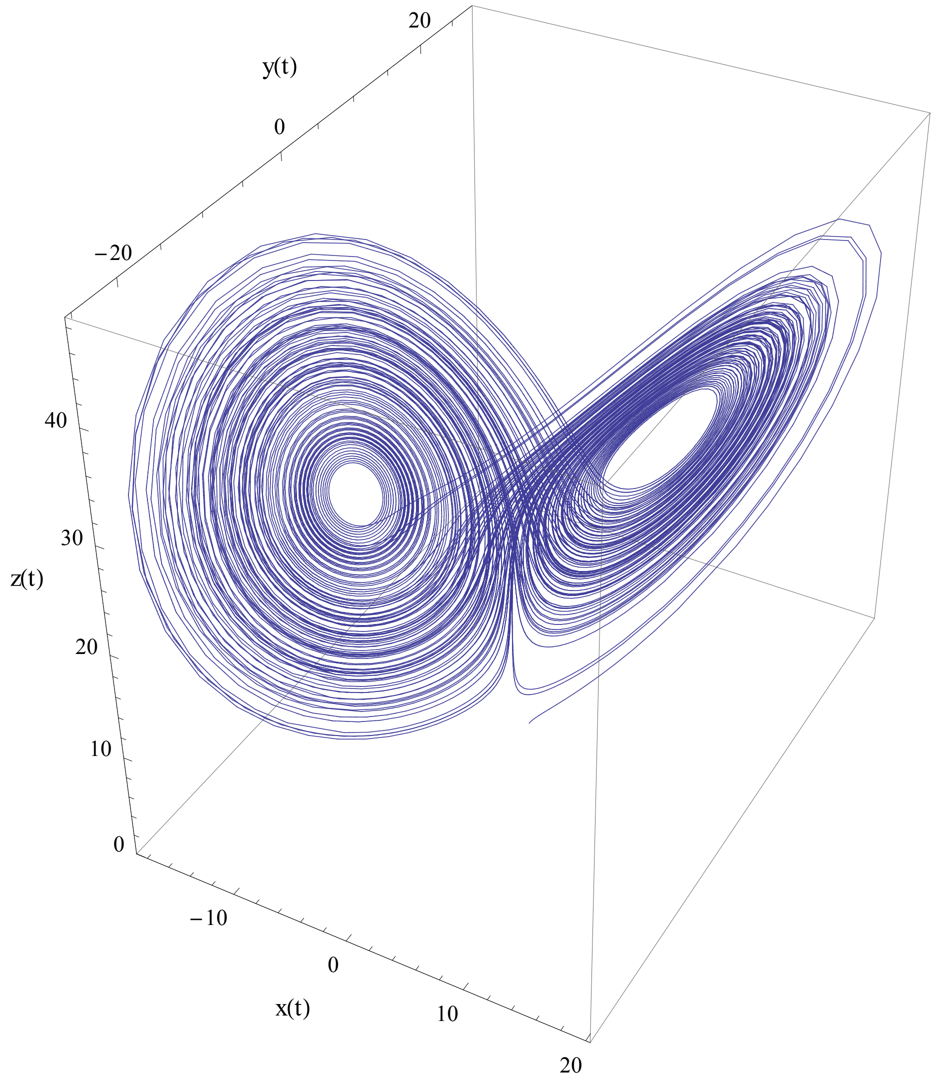

Figure 3: Parametric plot of Lorenz equations

the study of Lyapunov spectrum of the Lorenz equations. The typical values of the Lyapunov exponents for the Lorenz equations are $(1.50, 0, -22.46)$ for $\sigma = 10, b = \frac{8}{3}$ and $r = 28$. The exponents are computed in base e.

3.3 Scaling Of Chaotic Vector Fields

An ellipsoid with non uniform translaional inertia in the direction of its principal axes, is excited by a chaotic vector field, the Lorenz equations in this case, with respect to body fixed frame of reference. Consequently, the momentum vectors can

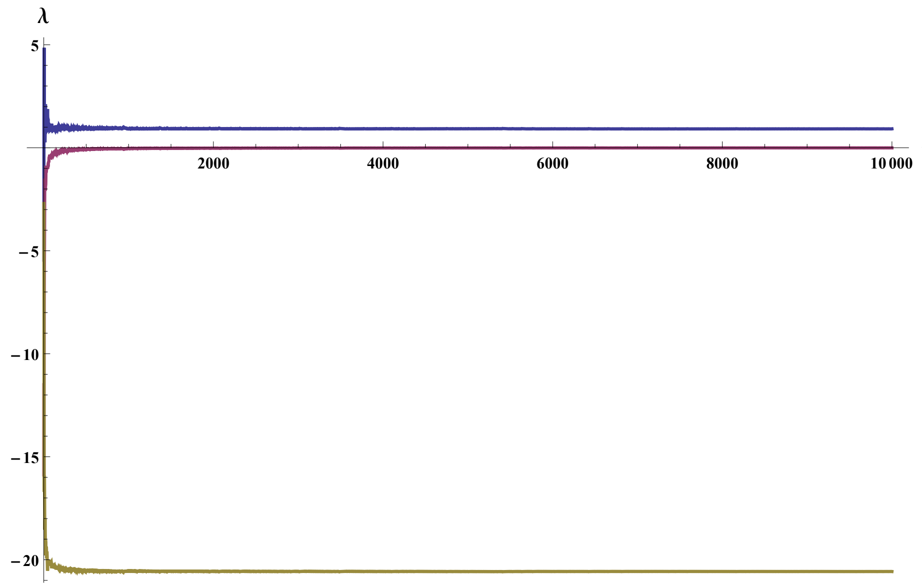

Figure 4: Lyapunov spectrum

expressed in body fixed coordinates as

$$M_1\dot{x} = \sigma(y - x) \tag{3.3.1a}$$

$$M_2\dot{y} = x(r - z) - y \tag{3.3.1b}$$

$$M_3\dot{z} = xy - bz. \tag{3.3.1c}$$

The components of the vector field on the right hand side of the differential equations are scaled by their respective translational inertia terms. The parameters σ, b and r are set at the the usual values of 10, $\frac{8}{3}$ and 28 for the purpose of simulation.

3.3.1 Variation in M_1 and M_2

The Lyapunov spectrum for the Lorenz equations are plotted for a range of values of M_1, while M_2 and M_3 are set at unity. The value of M_1 is incremented in steps of 0.025 from an intial value set at 1. The plot of the Lyapunov spectrum indicate that the strange attractor undergoes change in its topology of the phase space at around

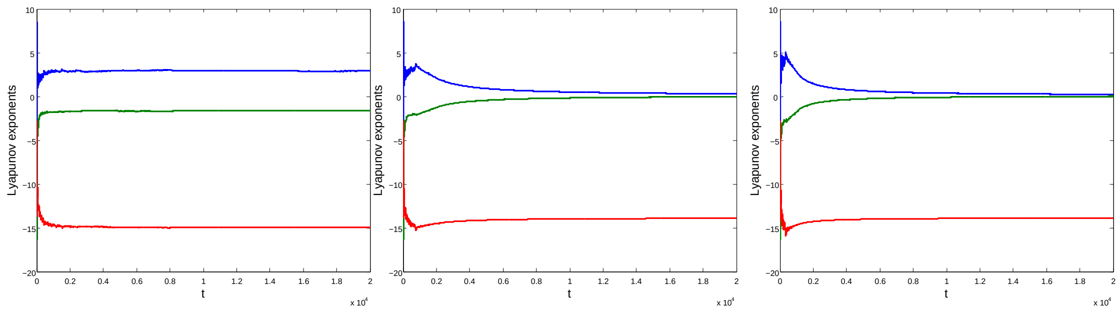

(a) $M_1 = 1.83$ (b) $M_1 = 2.00$ (c) $M_1 = 2.30$

Figure 5: Lyapunov spectrum for Lorenz system

$M_1 = 1.9$ and disappears completely. The largest Lyapunov exponent then rapidly converges to zero (Figures 3-5).

The Lyapunov spectrum for Lorenz equations are studied for variations in M_2 values, with M_1 and M_3 kept constant at unity. The departure of the chaotic nature of the flow of the vector field is observed for approximate value of $M_2 = 1.45$. The largest Lyapunov exponent collpases to zero, the rate of convergence of which increases with increase in M_2 value (Figures 4-6).

The plot of the solution curves indicate the break down of the strange attractor into two attracting fixed points. In case of $M_1 = 2$, an orbit with initial condition $(1, 1, 1)$ spirals into the fixed point C^2 (Fig.7). The pattern is repeated in case of $M_2 = 1.45$.

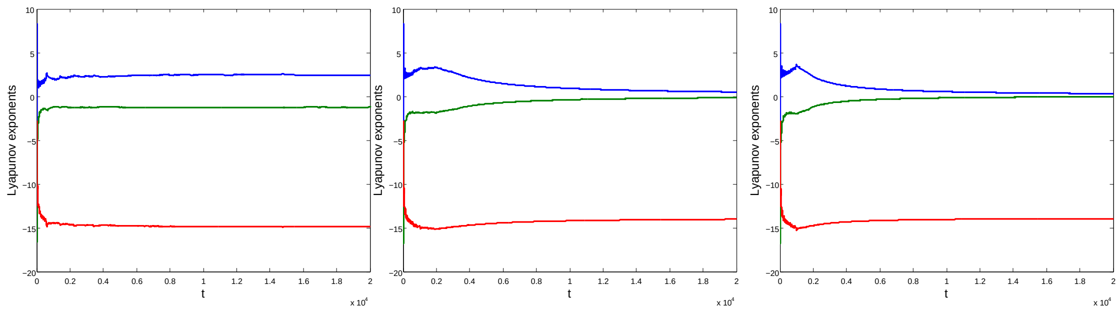

(a) $M_2 = 1.25$ (b) $M_2 = 1.45$ (c) $M_2 = 1.5$

Figure 6: Lyapunov spectrum for Lorenz system

3.3.2 Lorenz map

The Lorenz equations is an instance of deterministic chaos. Lorenz was able to extract the order of chaos by constructing the Lorenz map. In order to construct the map, the $z(t)$ data sequence is initially obtained from numerical integration of the differential equations. The set of local *maxima* of the sequence is then extracted by identifying the peaks. The Lorenz map is the plot of every $z(t)$ data point against its preceding value. The map is a spread of data points, even though it has the appearance of a smooth curve. Lorenz conjectured that since $z_{n+1} = f(z_n)$, it is possible to predict the dynamics of the system by forward iteration of the present z-value. The construction enabled Lorenz to eliminate the possibility of existence of stable limit cycles. As the slope of the curve is $|f'(z)| > 1$ everywhere, except for one point where the curve intersect the line of slope unity, existence of stable limit cycles can be effectively ruled out (Fig.6). The point of intersection z_n corresponds to a closed orbit as $z_{n+p} = z_n$ for some p. It may be proved, by applying linearization method, that small perturbations around z_n tend to grow monotonically [31].

The Lorenz maps were plotted for M_1 and M_2 values corresponding to $1.83, 2.00, 2.30$ and $1.25, 1.45, 1.50$, respectively. The map loses its coherent structure and the slope of the curve does not exhibit the property $|f'(z)| > 1$ for $M_1 \geq 1.99$ and $M_2 \geq 1.45$ (Fig.9-10). This fact implies the possibility of existence of stable limit cycles, since $|f'(z) < 1|$.

As the inertia parameters are varied over a range of values, there exists a subset of inertia values for which the integral curves of flow of the vector field are no longer chaotic. The system behaves like linear filter in the sense that it has the ability to scale a chaotic vector field; the solution curves of the vector field after rescaling is nonchaotic.

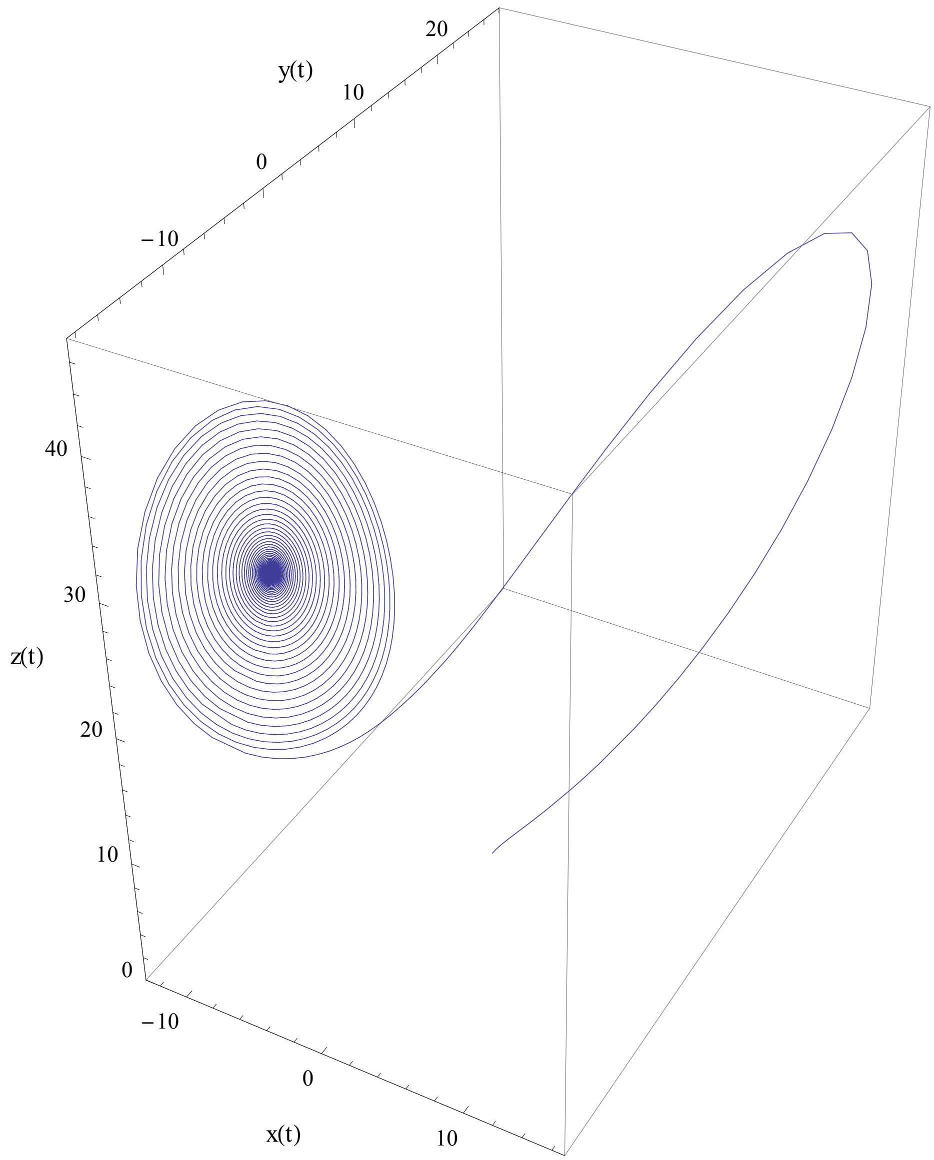

Figure 7: Parametric plot of Lorenz equations (M_1=2)

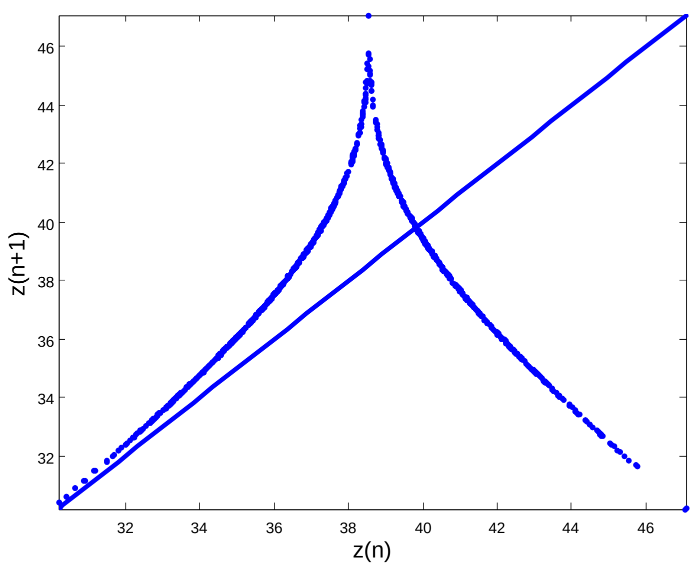

Figure 8: Lorenz map

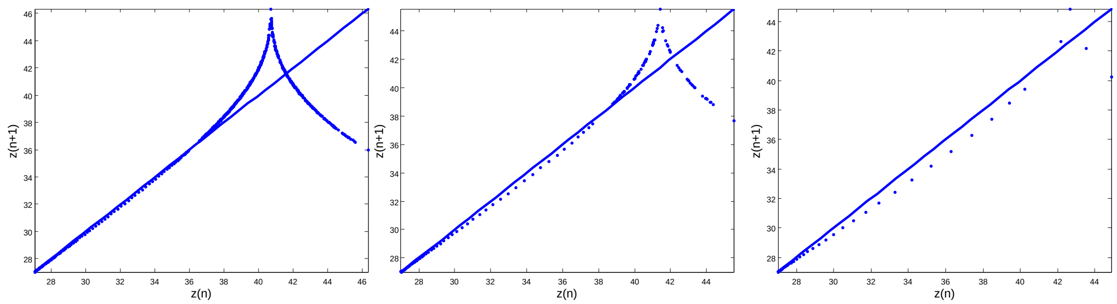

(a) $M_1 = 1.83$ (b) $M_2 = 1.2$ (c) $M_2 = 2.3$

Figure 9: Lyapunov spectrum for Lorenz system

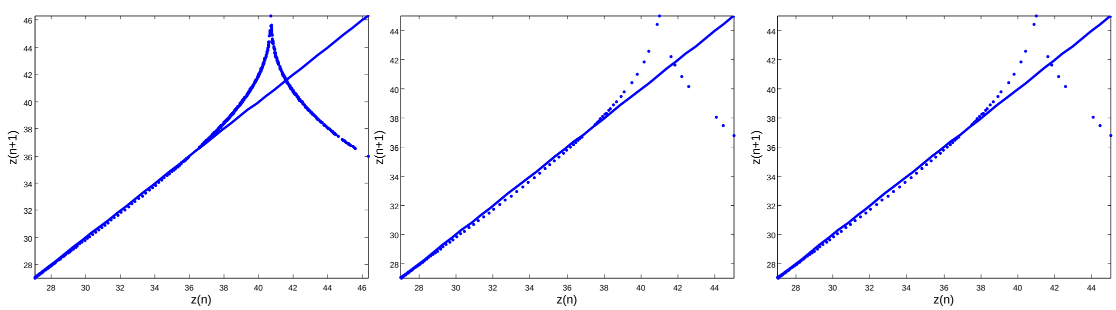

(a) $M_2 = 1.25$ (b) $M_2 = 1.45$ (c) $M_2 = 1.5$

Figure 10: Lyapunov spectrum for Lorenz system

CHAPTER 4: CHAOS IN NON-EUCLIDEAN SETTING

The investigation of chaos in the setting of configuration spaces that are non-Euclidean manifolds provides a resource for analyzing a wide range of dynamical systems that evolve on spaces other than $\mathbb{R}^n$. Vector fields assigned on Riemannian manifolds, are of common occurance while modeling physical systems. As an example, a mathematical model for ocean currents or atmospheric convection have the configuration space $\mathbb{S}^2$. The study of chaos in non-Euclidean manifolds involves determining the sensitivity of the system to small perturbations in initial conditions. The evaluation of finite-time Lyapunov exponents (FTLE) for spaces with different metrics, call for development of different computational strategies. A generalized numerical scheme for computation of FTLE and Lagrangian coherent structures to arbitrary Riemannian manifolds can be found in [17]. The scope of present research includes projecting the Lorenz vector fields onto $\mathbb{S}^3/\{0\}$ and investigating the nature of the vector field in terms of its Lyapunov exponents. The topological equivalence between the vector field defined by the ordinary differential equations that portrays the evolution of the Lorenz system on $\mathbb{S}^3/\{0\}$ and the vector field of the canonical Lorenz equations on $\mathbb{R}^3$, is examined. The study of chaotic systems is extended to other Riemannian manifold: the hyperbolic model (one of the models of hyperbolic geometry); the largest Lyapunov exponent being computed using the distance metric. Some of the definitions that will come up in course of stating the results are given as follows. The theoretical introduction to topology of vector fields is sourced from [32].

4.1 Equivalence Of Vector Fields

Let $f\colon M \to M$ and $g\colon N \to N$ be continuous functions defined on oriented manifolds M and N, respectively. The functions f and g are *topologically conjugate*, if there exists a homeomorphism $h\colon M \to N$, such that $h \circ f = g \circ h$. The following diagram commutes for topologically conjugate functions:

$$\begin{array}{ccc} M & \xrightarrow{f} & M \\ {\scriptstyle h}\downarrow & & \downarrow{\scriptstyle h} \\ N & \xrightarrow[g]{} & N \end{array} .$$

If h is r-times differentiable, then f and g are C^r-conjugate.

The notion of *topological equivalence* follows from the definition of topological conjugacy. The two vector fields $X_1 \in \mathfrak{X}(M)$ and $X_2 \in \mathfrak{X}(N)$ on M and N are topologically equivalent, if there exists a homeomorphism $h\colon M \to N$, which maps orbits in M to orbits in N,

$$h(\phi_t^1(x)) = \phi_t^2(h(x)) \tag{4.1.1}$$

for $x \in M$; ϕ_t^1 and ϕ_t^2 being the flows of the vector fields X_1 and X_2 respectively.

Definition 4.1.1. An orbit γ of a vector field X is positively (or negatively) stable if for any point $p \in \gamma$ and $\epsilon > 0$, there exists a real $\delta(p, \epsilon)$, such that, if $||q-p|| < \delta$, then the positive (or negative) semi-orbit of X through the point q lies within ϵ distance of the positive (or negative) semi-orbit of X passing through p.

In other words, if nearby orbits of γ of X stay in the neighborhood of γ in positive time, then the orbit γ is *positively stable*.

Definition 4.1.2. An orbit is positively (or negatively) unstable if it is not positively (or negatively) stable.

Definition 4.1.3. An orbit is is singular if it is unstable, or if it is an equilibrium.

In cases of vector fields on $\mathbb{S}^2$ that have finite number of singular points, the singular orbits are either

1. the equilibria or,
2. the separatrices of hyperbolic sectors at equilibria or,
3. isolated closed orbits.

The theorem on *topological equivalence* of a class of vector fields on $\mathbb{S}^2$ with polynomial vector fields can be stated in the following manner.

Theorem 4.1.4. Let X be a C^1 vector field on $\mathbb{S}^2$, such that,

1. no open subset of $\mathbb{S}^2$ is the union of closed orbits of $\mathbb{S}^2$;
2. X has finite number of singular orbits and
3. X satisfies the separatrix cycle condition.

Then X is topologically equivalent to a polynomial vector field.

The theorem along with a non-constructive proof can be found in [29]. The vector fields that describe the evolution of the Lorenz equations on $\mathbb{R}^3$ are mapped onto the $\mathbb{S}^3$, embedded in $\mathbb{R}^4$, by an orientation preserving homeomorphism. The stereographic projection is employed to project orbits in $\mathbb{R}^3$ to $\mathbb{S}^3$. The topologies of the vector fields have been studied for the two manifolds with reference to Lyapunov exponents. The

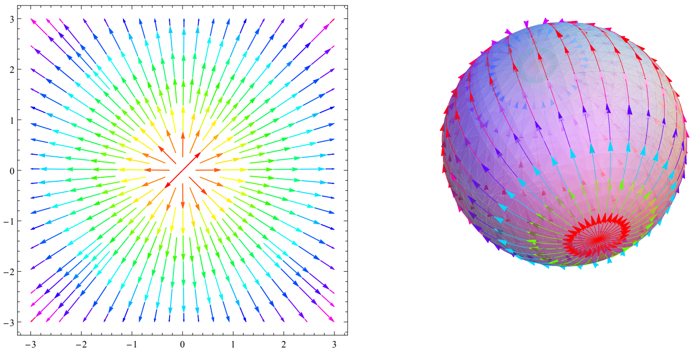

(a) Attractor on $\mathbb{R}^2$ (b) Attractor on $\mathbb{S}^2$

Figure 11: Attractor

influence of the metric and the homeomorphism on the qualitative behavior of the phase space is of special interest.

4.2 Stability Of Dynamical Systems On $\mathbb{S}^2$

The stability of a fixed point of a nonlinear autonomous system can be determined by the analysis of the linearized vector field about the point . This is true only if the conditions criteria in Theorem 2.1.5 is satisfied.

4.2.1 Limit sets on $\mathbb{S}^2$

A limit set on the 2-sphere can be one of the following types: fixed points, periodic orbits, quasiperiodic orbits and strange attractors. As part of the analysis, the flows of the vector fields for some of the limit sets, namely attractor, repeller, saddle and center on $\mathbb{R}^2$, are studied by projecting the vector fields stereographically onto $\mathbb{S}^2$ (Fig.11-14). It is worth noting that each fixed point in $\mathbb{R}^2$ gives rise to two fixed points in $\mathbb{S}^2$, indicating the fact that topological properties preserved locally and not globally.

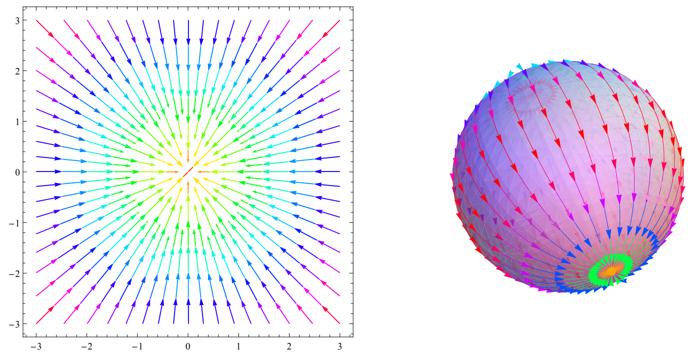

(a) Repeller on $\mathbb{R}^2$ (b) Repeller on $\mathbb{S}^2$

Figure 12: Repeller

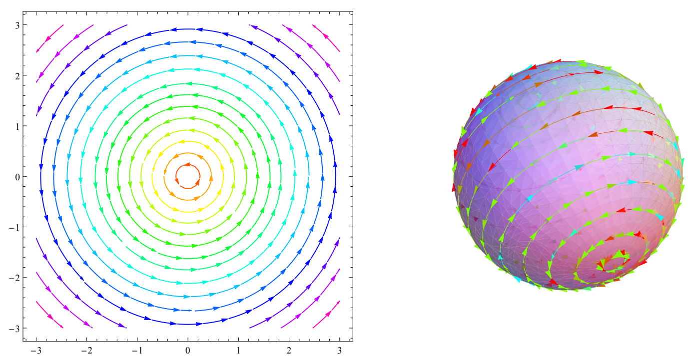

(a) Center on $\mathbb{R}^2$ (b) Center on $\mathbb{S}^2$

Figure 13: Center

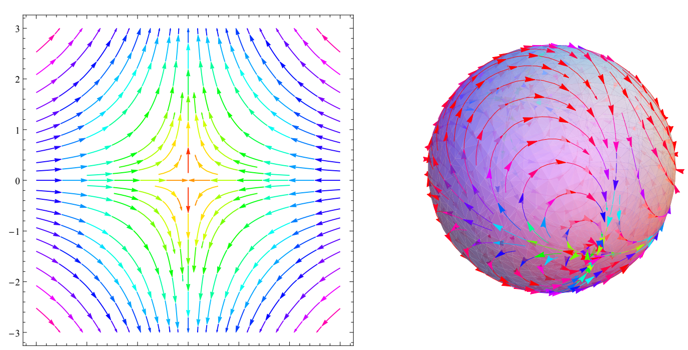

(a) Saddle point on $\mathbb{R}^2$ (b) Saddle point on $\mathbb{S}^2$

Figure 14: Saddle point

4.2.2 Bifurcations on $\mathbb{S}^2$

The study of topological structure of the flow or integral curve of a vector field enables characterization of the vector field in the study of stability of dynamical systems. The solutions of some differential equations display explicit dependence on parameters that are contained in the mathematical model of the system. Typically, a variation in the bifurcation parameter causes the flow to alter qualitatively about the fixed points. The Lorenz system is an example of a system that exhibits one-parameter family of bifurcations with change in the scalar r. One observes supercritical pitchfork bifurcation, subcritical Hopf bifurcation and a series of period doubling bifurcations as r varies over a range of values. The bifurcations of a dynamical system with one-parameter bifurcation are studied on $\mathbb{S}^2$ in the context of a homeomorphism. The bifurcations - saddle-node, transcritical, pitchfork and Hopf bifurcation are plotted on $\mathbb{S}^2$ by a conformal map in the following section. A detailed exposition of bifurcation theory can be found in [13].

1. Saddle-node bifurcation: A saddle-node bifurcation, also called a blue sky bifurcation, is a local bifurcation involving two fixed points that disappear after colliding with each other. A prototypical example of a system involving saddle-node bifurcation is

$$\dot{x} = \alpha + x^2 \tag{4.2.1a}$$

$$\dot{y} = -y. \tag{4.2.1b}$$

The parameter α is varied from -1 to 1. The system has two fixed points $(1, 0)$

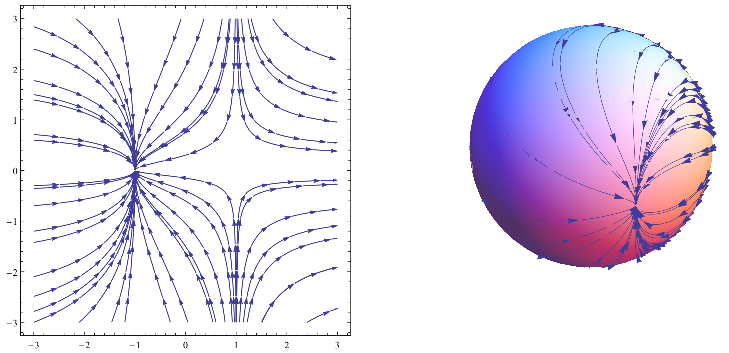

(a) Streamlines on $\mathbb{R}^2$ (b) Streamlines on $\mathbb{S}^2$

Figure 15: Saddle node bifurcation ($\alpha = -1$)

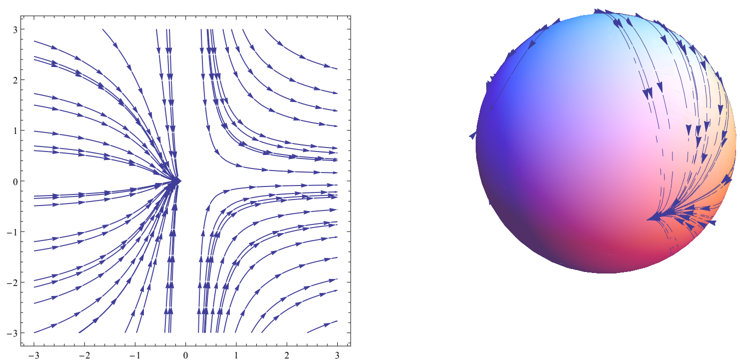

(a) Streamlines on $\mathbb{R}^2$ (b) Streamlines on $\mathbb{S}^2$

Figure 16: Saddle node bifurcation ($\alpha = 0$)

and $(-1, 0)$ for $\alpha = -1$. The first one is an attractor with eigenvalues -1 and -2, where as the second fixed point is a saddle with eigenvalues 2 and -1. As α is increased, the fixed points disappear for $\alpha > -1$ and there are no real fixed points (Fig.15-17).

2. Transcritical bifurcation: A transcritical bifurcation is one in which fixed points exchange their stability. The fixed points of the system exist for all range of

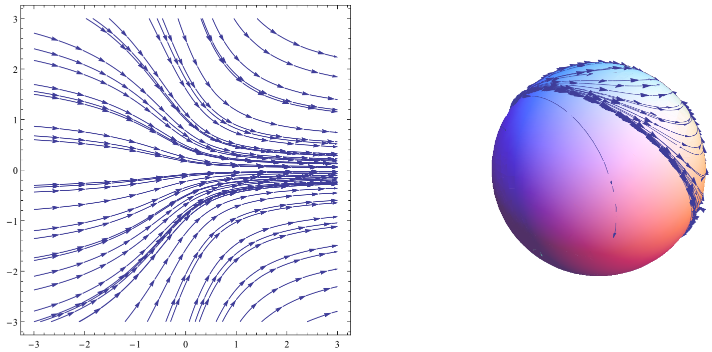

(a) Streamlines on $\mathbb{R}^2$ (b) Streamlines on $\mathbb{S}^2$

Figure 17: Saddle node bifurcation ($\alpha = 1$)

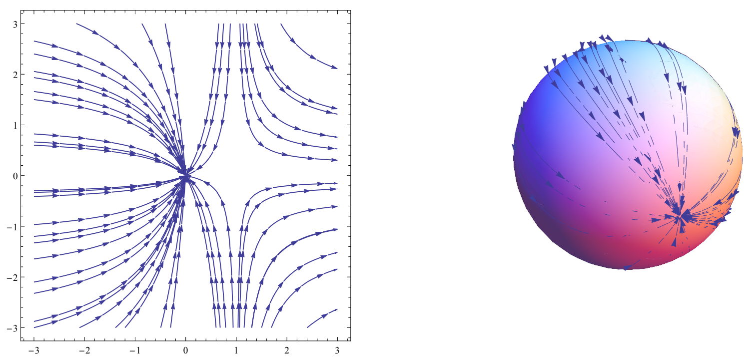

(a) Streamlines on $\mathbb{R}^2$ (b) Streamlines on $\mathbb{S}^2$

Figure 18: Transcritical bifurcation ($\alpha = -1$)

parameters. A typical example of transcritical bifurcation is given by

$$\dot{x} = \alpha x + x^2 \tag{4.2.2a}$$

$$\dot{y} = -y. \tag{4.2.2b}$$

The fixed points are an attractor at $(0, 0)$ and a saddle at $(1, 0)$, for $\alpha = -1$. The fixed points switch their stability as the value of α goes from -1 to 1 (Fig.18-20).

3. Pitchfork bifurcation: Pitchfork bifurcations occur in one of the two modes:

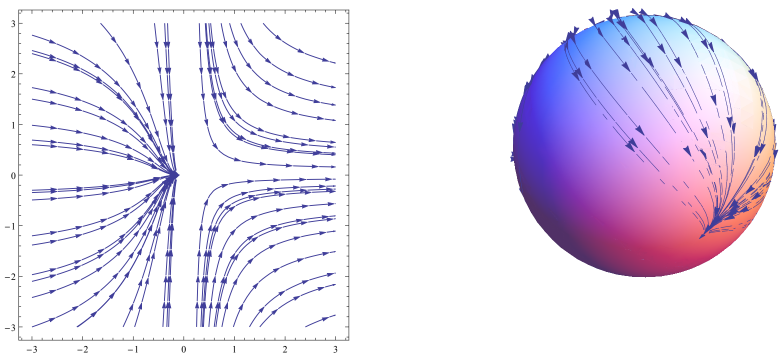

(a) Streamlines on $\mathbb{R}^2$ (b) Streamlines on $\mathbb{S}^2$

Figure 19: Transcritical bifurcation ($\alpha = 0$)

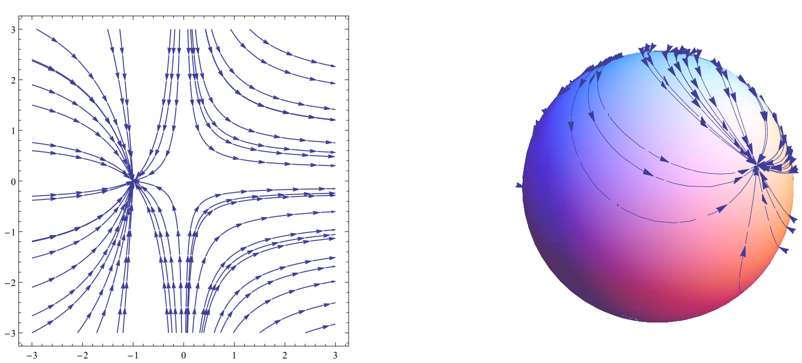

(a) Streamlines on $\mathbb{R}^2$ (b) Streamlines on $\mathbb{S}^2$

Figure 20: Transcritical bifurcation ($\alpha = 1$)

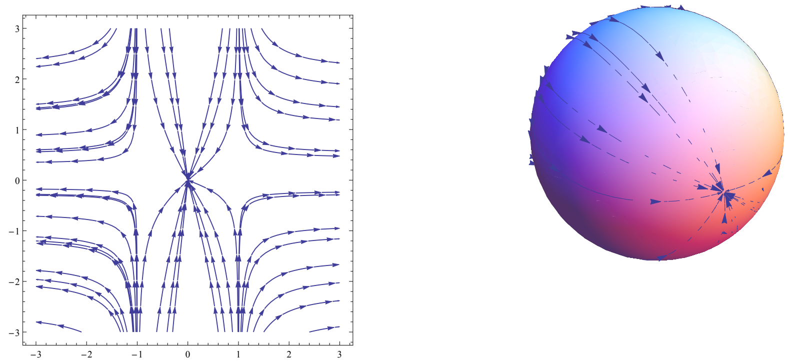

(a) Streamlines on $\mathbb{R}^2$ (b) Streamlines on $\mathbb{S}^2$

Figure 21: Supercritical pitchfork bifurcation ($\alpha = -1$)

supercritical and subcritical. A supercritical pitchfork bifurcation is one where the fixed point loses its stability, giving rise to two additional fixed points, as the bifurcation parameter is varied. Consider the two-dimensional dynamical system

$$\dot{x} = \alpha x - x^3 \tag{4.2.3a}$$

$$\dot{y} = -y. \tag{4.2.3b}$$

A supercritical pitchfork bifurcation takes place in x-y configuration space as α is turned up from -1 to 1 (Fig.21-23).

In case of subcritical pitchfork bifurcation, two stable saddle points collide as the value of the critical parameter α passes from -1 to 1, causing the orbit to collapse. A second order set of differential equations that yield subcritical

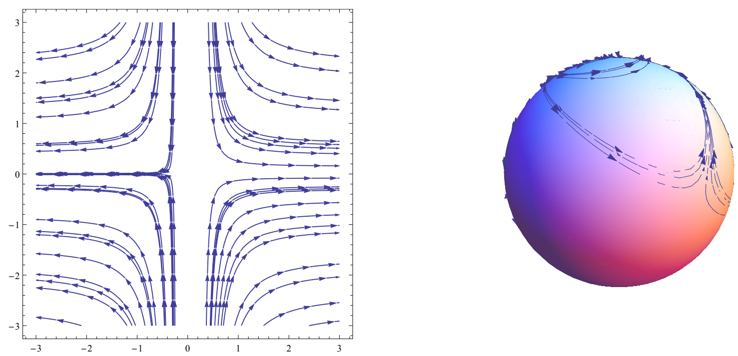

(a) Streamlines on $\mathbb{R}^2$ (b) Streamlines on $\mathbb{S}^2$

Figure 22: Supercritical pitchfork bifurcation ($\alpha = 0$)

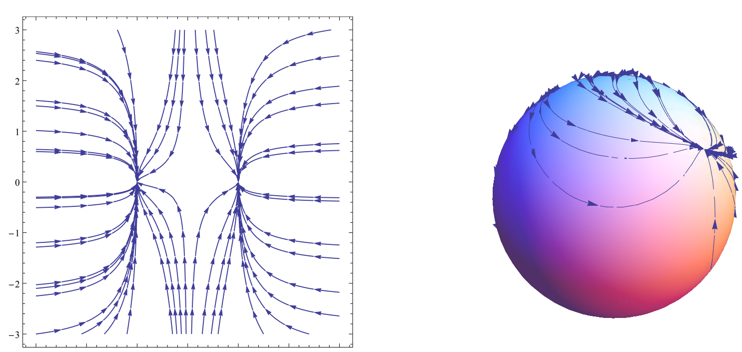

(a) Streamlines on $\mathbb{R}^2$ (b) Streamlines on $\mathbb{S}^2$

Figure 23: Supercritical pitchfork bifurcation ($\alpha = 1$)

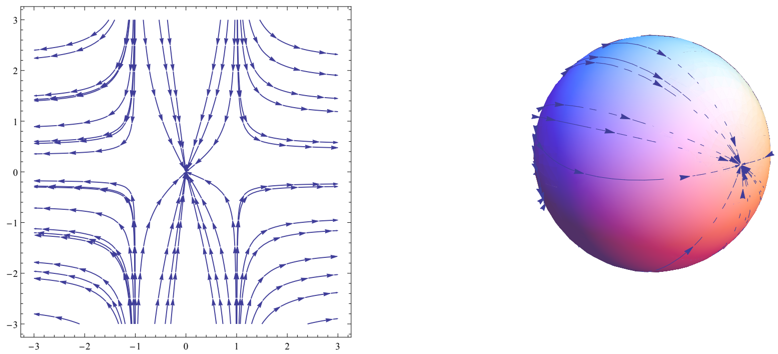

(a) Streamlines on $\mathbb{R}^2$ (b) Streamlines on $\mathbb{S}^2$

Figure 24: Subcritical pitchfork bifurcation ($\alpha = -1$)

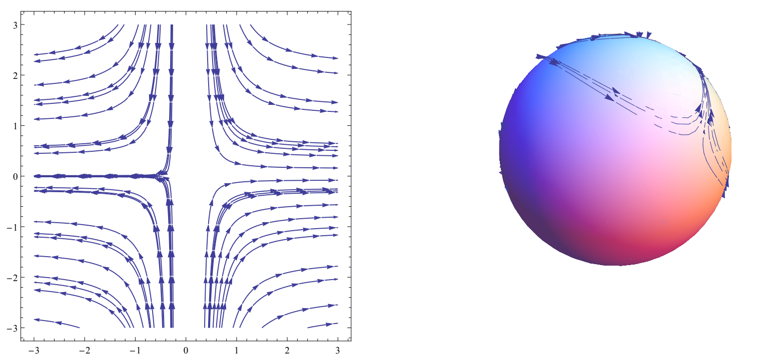

(a) Streamlines on $\mathbb{R}^2$ (b) Streamlines on $\mathbb{S}^2$

Figure 25: Subcritical pitchfork bifurcation ($\alpha = 0$)

pitchfork bifurcation is given by,

$$\dot{x} = \alpha x + x^3 \tag{4.2.4a}$$

$$\dot{y} = -y \tag{4.2.4b}$$

The plots (Fig.24-26) show the the flow of the vector fields with change in parameter α.

4. Hopf bifurcation: Hopf bifurcation occurs in two modes - supercritical and

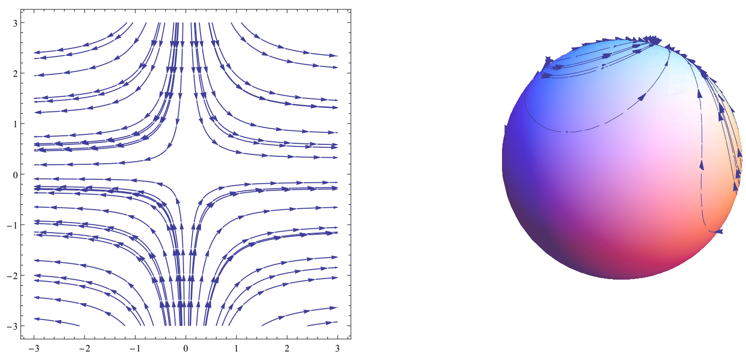

(a) Streamlines on $\mathbb{R}^2$ (b) Streamlines on $\mathbb{S}^2$

Figure 26: Subcritical pitchfork bifurcation ($\alpha = 1$)

subcritical. A system that undergoes subcritical Hopf bifurcation is

$$\dot{x} = -y + x(\alpha + (x^2 + y^2)) \tag{4.2.5a}$$

$$\dot{y} = x + y(\alpha + (x^2 + y^2)). \tag{4.2.5b}$$

The eigenvalues of the linearized differential equations about the fixed point $(0, 0)$ are $\alpha + i$ and $\alpha - i$. The fixed point is a hyperbolic fixed point for negative real part of the eigen values — the limit set of the system being a attractor. As α increases to positive range of values, the fixed point loses stability and switches to a repelling limit set (Fig.27-29).

A generic set of differential equations for subcritical Hopf bifurcation is

$$\dot{x} = -y + x(\alpha - (x^2 + y^2)) \tag{4.2.6a}$$

$$\dot{y} = x + y(\alpha - (x^2 + y^2)). \tag{4.2.6b}$$

The origin is a hyperbolic attractor for $\alpha < 0$: the eigenvalues of the linearized system at the fixed point being $-\alpha + i$ and $-\alpha - i$. The origin switches to a

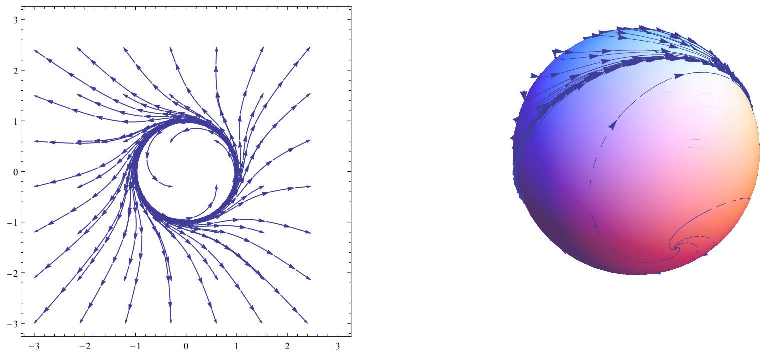

(a) Streamlines on $\mathbb{R}^2$ (b) Streamlines on $\mathbb{S}^2$

Figure 27: Supercritical Hopf bifurcation ($\alpha = -1$)

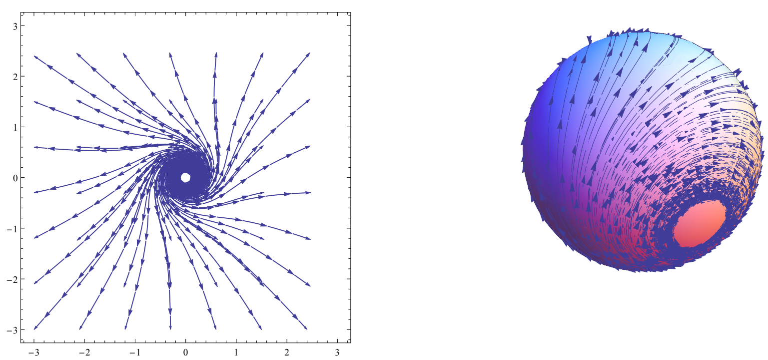

(a) Streamlines on $\mathbb{R}^2$ (b) Streamlines on $\mathbb{S}^2$

Figure 28: Supercritical Hopf bifurcation ($\alpha = 0$)

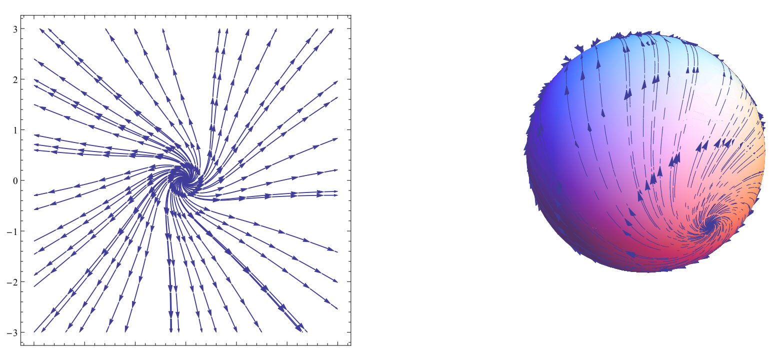

(a) Streamlines on $\mathbb{R}^2$ (b) Streamlines on $\mathbb{S}^2$

Figure 29: Supercritical Hopf bifurcation ($\alpha = 1$)

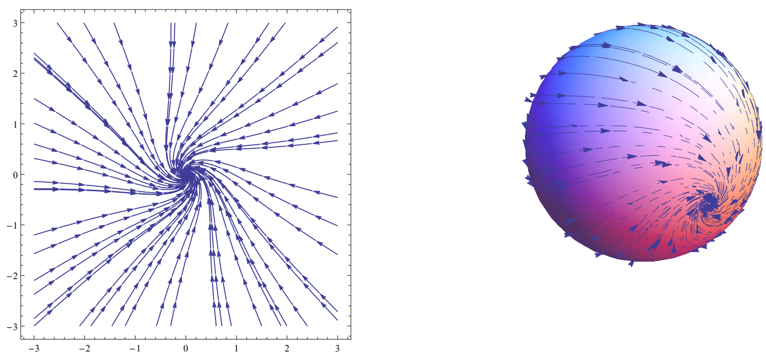

(a) Streamlines on $\mathbb{R}^2$ (b) Streamlines on $\mathbb{S}^2$

Figure 30: Subcritical Hopf bifurcation ($\alpha = -1$)

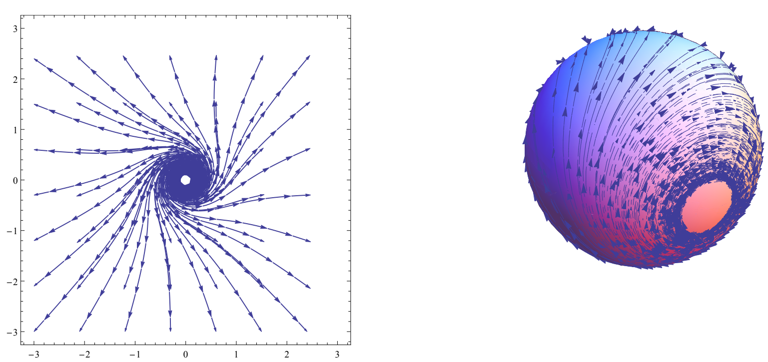

(a) Streamlines on $\mathbb{R}^2$ (b) Streamlines on $\mathbb{S}^2$

Figure 31: Subcritical Hopf bifurcation ($\alpha = 0$)

repeller and a stable limit attracting cycle appears. (Fig.30-32).

4.2.3 Bifurcation of the Lorenz system in $\mathbb{S}^3$

The Lorenz system in $\mathbb{R}^3$ exhibits pitchfork bifurcation when the value of the parameter r crosses 1. The globally stable fixed point at the origin loses its stablity and splits into two stable equilibrium points. The newly formed equilibria emerge close to the origin and migrate away from it as r is turned up (Figure 23a). The bifurcation curve appears to be the mirror image of its counterpart in $\mathbb{R}^3$. This can be attributed

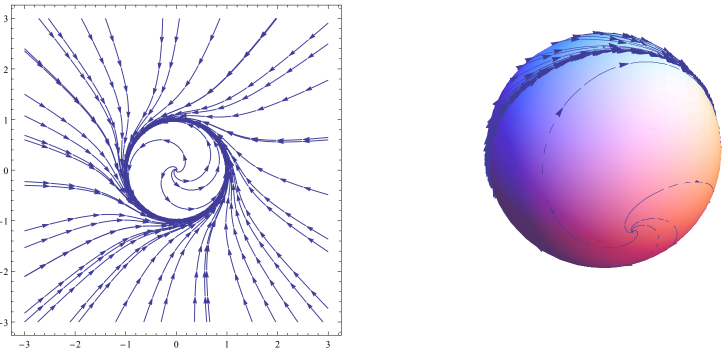

(a) Streamlines on $\mathbb{R}^2$ (b) Streamlines on $\mathbb{S}^2$

Figure 32: Subcritical Hopf bifurcation ($\alpha = 1$)

to the fact that the stereographic projection maps points in $\mathbb{R}^3$, that are close to the origin, to points in $\mathbb{S}^3$ that are further away from it (Fig.33b).

1 Equivalence of vector fields in $\mathbb{S}^3$ and $\mathbb{R}^3$

Let $X(x_1, x_2, x_3)$ be C^1 vector field on $\mathbb{R}^3$. The push-forward of the vector field, the stereographic projection map

$$X_1 = \frac{2x_1}{x_1^2 + x_2^2 + x_3^2 + 1}$$

$$X_2 = \frac{2x_2}{x_1^2 + x_2^2 + x_3^2 + 1}$$

$$X_3 = \frac{2x_3}{x_1^2 + x_2^2 + x_3^2 + 1}$$

$$X_4 = \frac{x_1^2 + x_2^2 + x_3^2 - 1}{x_1^2 + x_2^2 + x_3^2 + 1},$$

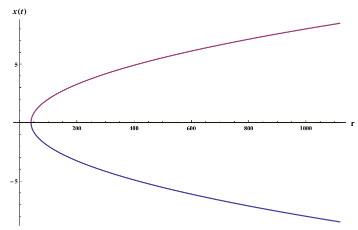

(a) Pitchfork bifurcation on $\mathbb{R}^3$

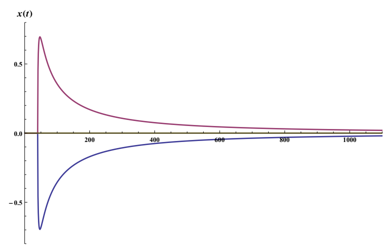

(b) Pitchfork bifurcation on $\mathbb{S}^2$

Figure 33: Lorenz bifurcation on $\mathbb{R}^3$ and $\mathbb{S}^2$

maps the the vector field onto the sphere $\mathbb{S}^3/(0,0,0,1)$. The invertible projection map is smooth and is

$$x_1 = \frac{X_1}{(1-X_4)}$$
$$x_2 = \frac{X_2}{(1-X_4)}$$
$$x_3 = \frac{X_3}{(1-X_4)}.$$

The derivative of the projection map restricts the C^1 vector field to $\mathbb{S}^3/(0,0,0,1)$, mapping the origin $\{0,0,0,0\}$ to $\{0,0,0,-1\}$. If the vector field X satisfies the conditions of Theorem 4.1.4, the projection map preserves the topological properties of the vector fields. Then a topologically equivalent vector field $\hat{X}$ can be defined on $\mathbb{S}^3$ in line with the theory of topologically equivalent vector fields [29]. The pull back of the vector field $\hat{X}$ on $\mathbb{R}^3$, by multiplication by suitable power of $x_1^2+x_2^2+x_3^2$, is a polynomial vector field. $\hat{X}$ and X are topologically equivalent.

4.3 Lyapunov Spectrum Of Lorenz System On $\mathbb{S}^3$

The Lorenz equations are mapped onto the manifold $\mathbb{S}^3/\{0\}$ via the push forward of the stereographic projection. As $\mathbb{S}^3$ is an embedded submanifold of $\mathbb{R}^4$, the vector fields are expressed in terms quadruplet of rectangular coordinates. The manifold $\mathbb{S}^3$ being a manifold of dimension 3, the vector field is written in terms of spherical coordinates by transformation of coordinates from $\mathbb{R}^4$ to $\mathbb{S}^3$. It is pertinent to keep in mind that the Lorenz spectrum is three dimensional with three Lyapunov exponents along the coordinate directions. The computation of Lyapunov exponents in $\mathbb{S}^3$ provides a basis for comparison of Lyapunov exponents between Lorenz vector fields in $\mathbb{R}^3$ and $\mathbb{S}^3$. A choice of spherical coordinates enables the components of the vector fields to lie on the tangent plane at each point on the manifold, with no component pointing to the outward direction normal to $\mathbb{S}^3$. The Lyapunov exponents are evaluated by computing the derivative of the vector field and then solving a system of coupled differential equations. The method has been described in detail in chapter 2. The Lyapunov spectrum plot indicate that the Lyapunov exponents on the $\mathbb{S}^3$ is identical to the one on $\mathbb{R}^3$. The steady state values of the three exponents are $0.92, 0$ and -20.55, which are the acceptable values for the Lorenz equations in $\mathbb{R}^3$.

The flow maps of the Lorenz vector field $\phi_t^1\colon \mathbb{R}^3 \to \mathbb{R}^3$ and $\phi_t^2\colon \mathbb{S}^3 \to \mathbb{S}^3$ are C^r diffeomorphisms. The stereographic projection $h\colon \mathbb{R}^3 \to \mathbb{S}^3$ is a C^k diffeomorphism where $r \leq k$. By definition, the flow maps ϕ_i^1 and ϕ_t^2 are C^k conjugate if the following diagram commutes:

$$\begin{array}{ccc} \mathbb{R}^3 & \xrightarrow{\phi_t^1} & \mathbb{R}^3 \\ h\downarrow & & \downarrow h \\ \mathbb{S}^3 & \xrightarrow[\phi_t^2]{} & \mathbb{S}^3 \end{array} .$$

The maps ϕ_t^1 and ϕ_t^2 are topologically conjugate if $k = 0$. The orbits of ϕ_t^1 get mapped to orbits of ϕ_t^2 by a diffeomorphism h if ϕ_t^1 and ϕ_t^2 are C^k conjugate. Morever, the eigenvalues of the derivative of the map $D(\phi_t^1(x_0))$ at any fixed point $x_0 \in \mathbb{R}^3$ are equal to the eigenvalues of $D(\phi_t^2(h(x_0)))$ [32]. The three critical points of the Lorenz attractor on $\mathbb{S}^3$ are $(0, 0, 0, -1)$, $(0.019, 0.019, 0.062, 0.1)$ and $(-0.019, -0.019, 0.062, 0.099)$. The eigenvalues of the linearized set of equations around the fixed points yield the eigenvalues $(-22.828, 11.828, -2.667, 0)$, $(-13.855, 0.094+10.195i, 0.094+10.195i, -1.048\times 10^{-13})$ and $(-13.855, 0.094 + 10.195i, 0.094 + 10.195i, -1.048 \times 10^{-13})$ respectively. The sets of eigenvalues are the same as that of the linearized Lorenz equations on $\mathbb{R}^3$, about the fixed points. The fact that the Lyapunov exponents remain the same for both manifolds indicate an identical local rate of stretching and folding of the configuration spaces in both cases.

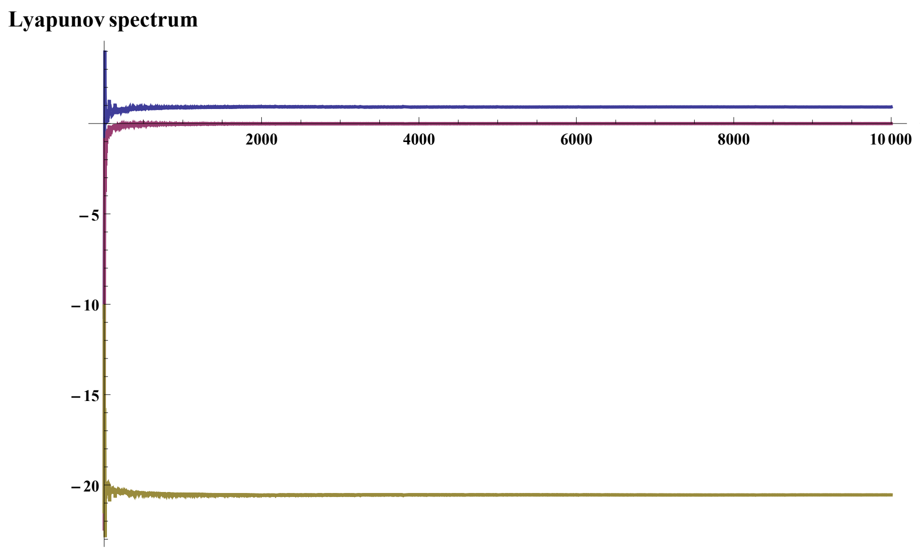

Figure 34: Lyapunov spectrum for Lorenz system on 3-sphere

CHAPTER 5: REDUCTION IN MANIFOLDS

5.1 Lie Groups

Lie groups model continuous symmetry of mathematical objects. The importance of Lie groups lies in the fact that the configuration spaces of physical systems are Lie groups. A salient features of Lie group theory is outlined here.

Definition 5.1.1. (Lie groups) A Lie group is a C^∞ manifold that is also a group with

(i) smooth group operation, $G \times G \to G$ and

(ii) smooth inversion, $G \to G$.

More precisely, group operation and inversion are C^∞ maps of manifolds. For any element $g \in G$ the maps $L_g, R_g \colon G \times G \to G$, called the *left* and *right* translation respectively, are defined as

$$L_g(h) = gh \tag{5.1.1}$$

$$R_g(h) = hg \tag{5.1.2}$$

where $h \in G$. The inversion map is defined as $g \mapsto g^{-1}$.

Definition 5.1.2. (Lie group action) Given a smooth manifold M and a Lie group G, the left action of G on M is the map $\phi \colon G \times M \to M$, $\phi(g, q) \mapsto gq$ such that

(i) $\phi(g\phi(h, q)) = \phi(gh, q)$

(ii) $\phi(e, q) = q$

where $g, h \in G$, $q \in M$ and e is the identity elemnt.

The map g_M, defined as $\phi(g, .)$, is the group of diffeomorphism of M onto itself for each $g \in G$. The set of all such g_Ms can defined as

$$\rho \colon G \to \mathrm{Diff}(M) \tag{5.1.3}$$

$$g \mapsto g_M. \tag{5.1.4}$$

ρ is a group homomorphism that maps from the group G to the group of diffeomorphisms on M with the properties

(i) $\rho(e) = id_M$ and

(ii) $\rho(g_1)(g_2) = \rho(g_1)\rho(g_2)$.

where e is the group identity and $g_1, g_2 \in G$.

The action of a group G on a manifold M is called

1. transitive, if for any $x, y \in M$, $\exists g \in G$, such that $gx = y$,

2. free, $gx = x, \iff x = e$, the identity element,

3. effective or faithful, for any $g, h \in G$, $\exists x \in M$, such that $gx \neq hx$. Alternatively, $g \neq e \Rightarrow gx \neq x$.

Theorem 5.1.3. (Closed subgroup theorem) If H is a closed subgroup of a Lie group G, i.e. $H < G$, then,

(i) H is a Lie group with induced topology of G and

(ii) H is an embedded submanifold of G.

Definition 5.1.4. (Lie algebra) A Lie algebra $\mathfrak{g}$, is a vector space together with a bilinear bracket operation (called the Lie bracket), $[.,.]\colon \mathfrak{g} \to \mathfrak{g}$, which is

(i) skew symmetric, $[\xi, \eta] = -[\eta, \xi]$ and

(ii) satisfies the Jacobi identity, $[\xi, [\eta, \zeta]] + [\eta, [\zeta, \xi]] + [\zeta, [\xi, \eta]] = 0$

for $\xi, \eta, \zeta \in \mathfrak{g}$.

Given a Lie group G, it has an associative Lie algebra $\mathfrak{g} = T_e G$, which is the tangent space at the identity and is equipped with a bracket operation, called the Lie bracket that can be derived from the Jacobi-Lie bracket. In particular, if a Lie group is finite dimensional, the Lie algebra is a linear vector space of the same dimension.

Definition 5.1.5. (Left invariant vector field)A vector field X^L on a Lie group G is left inavriant if

$$T_h L_g(X^L) = X^L(L_g h); \forall g, h \in G. \tag{5.1.5}$$

The notion of reduction in physical systems is based on the famous Noether's theorem [23]. The symmetries of the system are exploited to compute the conserved integrals of motion of Hamiltonian systems. In particular, symmetries give rise to underlying conservation laws, thereby leading to reduction in configuration space. All conservation laws such as translational and rotational momentum, energy, arise from corresponding symmetries of the system. Subsequently, Noether's theorem has been formulated in the setting of symplectic and Poisson manifolds for systems that are Hamiltonian. A more detailed exposition on reduction of Poisson manifolds is available in [9] and for reduction in the symplectic setting as well, in [19]. The classical reduction in symplectic manifolds is due to the work of Marsden and Weinstein [20]. A significant work in the theory of Poisson reduction is the publication by Marsden and Ratiu [18].

5.2 Hamiltonian Dynamics In Symplectic Manifold

Let (M, ω) be a symplectic manifold with a closed and nondegenerate symplectic 2-form ω. The smooth action of a Lie group G on M is symplectic, if under the group action $\phi\colon G \times M \to M$, the symplectic form remains invariant under the pull-back of $\forall g \in G$,

$$\phi^{*}\omega = \omega. \tag{5.2.1}$$

A smooth action of G on a member $q \in M$ induces an equivalence class that consists of all points that lie in the orbit of q.

$$[q] := \{x \colon x \in Orb(q)\}. \tag{5.2.2}$$

A quotient space is the set of all orbits and is written as M/G. Let a surjective map be defined as

$$\pi\colon M \to M/G \tag{5.2.3}$$

such that $\pi(q) = [q] = Orb(q)$ for all $q \in M$. The quotient space inherits the quotient topology meaning, any $U \subseteq M/G$ is open, iff $\pi^{-1}U$ is open in M. An important result in the theory of reduction of smooth manifolds is the quotient manifold theorem.

Theorem 5.2.1. (Quotient manifold theorem) If a Lie group G acts on a manifold M by a group action $\phi\colon G \times M \to M$ that is free, smooth and proper, then the orbit space defined by M/G is a topological manifold equipped with a unique smooth structure. The quotient map $\pi\colon M \to M/G$ is a smooth submersion and the dimension of the quotient manifold is given by $dim(M) - dim(G)$.

An outcome of this theorem is the fact that all orbits are immersions in the quotient space. The additional fact that the group action is free and proper ensures that they are embedded submanifolds. The tangent space at the identity e is the Lie algebra $\mathfrak{g}$ of G. The dual of $\mathfrak{g}$, denoted by $\mathfrak{g}^*$, is related to $\mathfrak{g}$ by the natural pairing between the two,

$$\langle \xi, \alpha \rangle = \mathbb{R} \tag{5.2.4}$$

for $\xi \in \mathfrak{g}$ and $\alpha \in \mathfrak{g}^*$. The exponential map $exp\colon \mathfrak{g} \to G$ is $\gamma(t)$ is the time t flow along the one parameter subgroup of G,

$$\exp(t\xi) = \gamma(t) \tag{5.2.5}$$

satisfying $\gamma(0) = e$ and $\dot{\gamma}(t) = \xi$. $\gamma(t)$ is the flow of the left invariant vector field on G, generated by left translation of ξ. The action of the group G on M is given by the infinitesimal generator vector field on M for a Lie algebra element ξ is given as,

$$\xi_M(q) = \left.\frac{d}{dt}\right|_{t=0} \phi(\exp(t\xi), q) \tag{5.2.6}$$

for $q \in M$. An inner-automorphism on G can be defined as a map $I_g\colon G \to G$,

$$I_g h = (L_g \circ R_g^{-1})h = ghg^{-1} \tag{5.2.7}$$

for $g, h \in G$. The map I_g is map from G to the set of automorphisms Aut(G). The push-forward of I_g evaluated at the identity is the adjoint map, denoted by Ad_g,

$$Ad_g\xi = \left.\frac{d}{dt}\right|_{t=0} g.\exp(t\xi).g^{-1} = T_e I_g \xi \tag{5.2.8}$$

given $\xi \in \mathfrak{g}$. The adjoint map Ad_g represents the set of automorphisms $\mathrm{Aut}(\mathfrak{g})$ on the Lie algebra.

$$Ad_g \colon \mathfrak{g} \mapsto \mathrm{Aut}(\mathfrak{g}) \tag{5.2.9}$$

Given $g \in G$, the adjoint map can be viewed as a Lie algebra homomorphism from G to $\mathrm{Aut}(\mathfrak{g})$. The map

$$Ad \colon g \mapsto Ad_g \tag{5.2.10}$$

is a representation of G on the group $\mathrm{Aut}(\mathfrak{g})$ and is known as the adjoint representation of G. There exists a co-adjoint action of G on $\mathfrak{g}^*$ in manner similar to the adjoint action of G on $\mathfrak{g}$. The co-adoint action of G on $\mathfrak{g}^*$ is the inverse dual of its adjoint action and is given by $Ad^*_{g^{-1}}$,

$$\langle Ad^*_{g^{-1}}\alpha, \xi\rangle = \langle \alpha, Ad_{g^{-1}}\xi\rangle \tag{5.2.11}$$

for $\alpha \in \mathfrak{g}^*$ and $\xi \in \mathfrak{g}$.

Definition 5.2.2. (Momentum map) Let a Lie group G act on a symplectic manifold M by symplectic action $\phi \colon G \times M \to M$. Suppose there exists a function $J(\xi) \colon M \to \mathbb{R}$, which depends linearly on $\xi \in \mathfrak{g}$, such that

$$X_{J(\xi)} = \xi_M \tag{5.2.12}$$

$\forall \xi \in \mathfrak{g}$, then the map $\mathbb{J}\colon M \to \mathfrak{g}^*$ defined by,

$$< \mathbb{J}(q), \xi >= J(\xi)(q) \tag{5.2.13}$$

for $q \in M$ is called the momentum map for the group action ϕ.

A momentum map exists if a symplectic action gives rise to infinitesimal generator vector fields that are Hamiltonian.

5.2.1 Symplectic reduction

Let a Lie group G act symplectically on a symplectic manifold (M, ω). The action of G on M induces a momentum map $\mathbb{J}$ that is Ad^*-equivariant. A momentum map is Ad^*-equivariant, if $\mathbb{J}(\phi_g(q)) = Ad^*_{g^{-1}}(\mathbb{J}(q))$ for $g \in G$ and $q \in M$. The symplectic reduction involves two stages :

1. Let $\mu = \mathfrak{g}^*$ be a regular valued dual Lie algebra element. The evolution of the system happens over the level momentum set μ and the restricted manifold is given as $\mathbb{J}^{-1}(\mu)$. The inclusion map i_μ onto M is defined as

$$i_\mu\colon \mathbb{J}^{-1}(\mu) \to M. \tag{5.2.14}$$

2. The isotropy subgroup G_μ of G acts on elements of $\mathfrak{g}^*$ by the Ad^* action. The action is free, proper and leaves μ fixed. This action induces a restricted equivariant momentum map $\mathbb{J}_\mu\colon M_\mu \to \mathfrak{g}^*_\mu$. The dual Lie algebra $\mathfrak{g}^*_\mu$ is the reduced dual Lie algebra corresponding to G_μ. The group action G_μ is used for further reduction to get the reduced manifold by the quotient action $M_\mu = \mathbb{J}^{-1}(\mu)/G_\mu$. The manifold M_μ inherits a unique symplectic form ω_μ that is given

by,

$$\pi_\mu^* \omega_\mu = i_\mu^* \omega \tag{5.2.15}$$

where π_μ is the canonical projection map $\pi_\mu \colon \mathbb{J}^{-1}(\mu) \to M_\mu$.

5.3 Hamiltonian Dynamics In Poisson Manifold

A Poisson manifold is a manifold P along with a bracket operation $[\cdot, \cdot]$ and is designated by $(P, [\cdot, \cdot])$. A Poisson bracket is a derivation on the algebra $C^\infty(P)$ that is skew symmetric, distributive and obeys Leibniz rule. A Poisson algebra is the pair $(C^\infty, [\cdot, \cdot])$. Since there exists a natural isomorphism between vector fields on P and derivations on $C^\infty(P)$, for any $H \in C^\infty(P)$ there is a unique vector field X_H on P, which is given by the expression $X_H = \{\cdot, H\}$. X_H is called the Hamiltonian vector field for the Hamiltonian function H. The equations of motion of the system can be expressed in terms of the Poisson bracket. If ϕ_t be the flow of the Hamiltonian vector field X_H, then H is constant along ϕ_t. Then it follows that for any $F \in C^\infty(P)$,

$$\frac{d}{dt}\{F \circ \phi_t\} = \{F, H\} \circ \phi_t = \{F \circ \phi_t, H \circ \phi_t\} = \{F \circ \phi_t, H\}. \tag{5.3.1}$$

Alternatively, this can be written as $\dot{F} = \{F, H\}$. A function $G \in C^\infty(P)$ is a Casimir if $\{G, f\} = 0$ for any function $f \in C^\infty(P)$. The Casimir G is constant along the integral curves of the Hamiltonian vector field X_H, i.e., $\{G, H\} = 0$. The set of Casimir functions form the center $\mathfrak{C}(P)$ of the Lie algebra $(C^\infty(P), [\cdot, \cdot])$.

A smooth map $\Phi \colon P_1 \to P_2$ between two Poisson manifolds $(P_1, \{\cdot, \cdot\}_1)$ and $(P_2, \{\cdot, \cdot\}_2)$ is a Poisson map if $\Phi^*\{F, K\}_2 = \{\Phi^* F, \Phi^* K\}_1 \; \forall F, K \in C^\infty(P_2)$.

5.3.1 Poisson reduction

An action ϕ of a Lie group G on a Poisson manifold $(P, [\cdot,\cdot])$ is a map $\phi\colon G \times P \to P$. The map ϕ is canonical if for any $g \in G$ and $F, K \in C^\infty(P)$,

$$\{F, K\} \circ \phi_g = \{F \circ \phi_g, K \circ \phi_g\}. \tag{5.3.2}$$

If the group action ϕ_g is smooth, free and proper, then the orbit space P/G is a smooth regular quotient manifold and the projection $\pi\colon P \to P/G$ is a submersion. The submanifold P/G inherits a unique Poisson bracket $\{\cdot,\cdot\}_{P/G}$,induced by the projection map π, such that

$$\{F, K\}_{P/G} \circ \pi = \{F \circ \pi, K \circ \pi\} \tag{5.3.3}$$

for any $F, K \in C^\infty(P/G)$. The reduced Hamiltonian $h\colon P/G \to \mathbb{R}$ on P/G can be computed as $H = h \circ \pi$ for a G-invariant $H\colon P \to \mathbb{R}$. If ϕ be the flow of the Hamiltonian vector field X_H, then the flow of the reduced Hamiltonian vector field X_h is given as

$$\phi_{P/H} \circ \pi = \pi \circ \phi. \tag{5.3.4}$$

5.4 Principal Fiber Bundle

The canonical reduction methods on symplectic and Poisson manifolds with symmetry are powerful reduction techniques that can be extended to manifolds that are principal fiber bundles. The configuration spaces of the dynamical systems that are studied in this document are principal fiber bundles. The following material illustrates some key definitions and results on prinipal fiber bundles. An elaborate treatment on theorems and proofs on the subject can be found in [12] and [22].

Definition 5.4.1. (Fiber bundle) A fiber bundle is a manifold that is a quadruple (E, M, F, π), where E is the total space, M the base space, F the fiber space and π the projection map; $\pi\colon E \to M$.

A fiber bundle is differentiable if it is locally trivial. For any $x \in M$ there exists an open neighborhood U around x and a diffeomorphism ψ,such that $\psi\colon \pi^{-1}(U) \cong U \times F$, or in other words, the following diagram commutes:

$$\begin{array}{ccc} \pi^{-1}U & \xrightarrow{\psi} & U \times F \\ \downarrow \pi & \swarrow \pi_1 & \\ U & & \end{array} .$$

For any $u \in \pi^{-1}(U)$, $\pi(u) = \pi_1 \circ \psi(u)$, where π_1 is the projection on to the first component of U. The fiber over any $x \in M$ is denoted either by $\pi^{-1}(x)$ or F_x, and is homeomorphic to F. A bundle map between two fiber bundles (E_1, M_1, F_1, π_1) and (E_2, M_2, F_2, π_2) is the collection of maps $\tilde{f}\colon E_1 \to E_2$ and $f\colon M_1 \to M_2$, such that the following diagram commutes:

$$\begin{array}{ccc} E_1 & \xrightarrow{\tilde{f}} & E_2 \\ {\scriptstyle \pi_1}\downarrow & & \downarrow{\scriptstyle \pi_2} \\ M_1 & \xrightarrow[f]{} & M_2 \end{array} .$$

Two fiber bundles over the same base manifold M, E_1 and E_2, having the same fiber F, are isomorphic if the bundle map consisting of the maps, $\tilde{f}\colon E_1 \to E_2$ and the identity map $f\colon M \to M$ and is an isomorphism itself. A trivial fiber bundle is globally isomorphic to the product bundle $M \times F$.

A transition function enables comparison of coordinate charts in a neighborhood of an atlas of a manifold. The transition functions are defined on overlapping coordinate charts and are defined as inverse composition of local trivializations.

Definition 5.4.2. (Transition function) Let (E, M, F, π) be a smooth fiber bundle. Since, there exists a trivialization for any open cover U_α in M, $\psi_\alpha\colon \pi^{-1}(U_\alpha) \to U_\alpha \times F$; for any two adjacent open covers U_α and U_β, there is an isomorphism of F over U_α and U_β;

$$\psi_\alpha \circ \psi_\beta^{-1} = (U_\alpha \cap U_\beta) \times F \cong (U_\alpha \cap U_\beta) \times F \tag{5.4.1}$$

The map has the form, $\psi_\alpha \circ \psi_\beta^{-1}(b, p) \to b, g_{\alpha\beta}(p)$, for $b \in U_\alpha \cap U_\beta$ and $p \in F$; where $g_{\alpha\beta}$ is called transition function.

The transition functions belong to the set of all diffeomorphisms of the fibers on to themselves. When the subgroup of such diffeomorphisms is a Lie group G, such that G acts on F by the natural smooth map $G \times F \to F$, the Lie subgoup is called a structure group G. The actions of transition functions $g_{\alpha\beta}$ to the set of diffeomorphisms of F define smooth maps from $U_\alpha \cap U_\beta$ into a Lie transformation group G, which is a subset of the group of diffeomorphisms. In this case, $\{U_\alpha, \psi_\alpha\}$ defines a G structure in (E, π, M, F) with structure group G [7].

Definition 5.4.3. (Principal fiber bundle) Let G be a Lie group. A principal fiber bundle (right) is a manifold that is a quadruple (Q, M, G, π), where Q is the total space, M the base space, G the fiber space and π the projection map, $\pi\colon Q \to M$, satisfying the following conditions:

1. G acts on itself by left translation, that is, $L_g\colon h \mapsto gh$, where $g, h \in G$
2. M is the quotient space of Q induced by the equivalence relation, $M = Q/G$.

An action (left) of the group G on the principal bundle Q is the map $Q \times G \to Q$

and is defined as $(x,h)g \to (x,gh)$ for $x \in M$ and $g,h \in G$. The action is free, meaning, if $(x,h)g = (x,h)$, then $g = e$, the identity element.

5.5 Connection

In general, there is no natural way of comparing tangent vectors that belong to different fibers in a fiber bundle. A connection is a construct that enables one to relate tangent vectors along fibers on separate base points. Relatedly, a connection on a fiber bundle makes it possible to compute parallel transport, a map that describe the way tangent vectors move along a curve on the base manifold. The theory on connection and parallel transport has been sourced from [22].

Definition 5.5.1. (Ehresmann connection) Let (E, M, F, π) be a smooth fiber bundle, where E is the total space, M the base space, F the fiber space and π the projection map. An Ehresmann connection is an assignment of a vertical subspace V_u of the tangent space T_uE, at each point $u \in E$, such that, V_u is the complement of the direct sum decomposition of the tangent space with the horizontal subspace H_u.

Vectors that are tangent to the fiber are 'naturally' identified with vertical vectors. However, there is no natural identification of horizontal vectors. Ehresmann connection (generalized Cartan connection) provide a basis for decomposition of the tangent space of the fiber bundle at each point in the manifold. The tangent space T_uE can be written as $T_uE = T_uM \oplus T_uF$. The vertical subspace is given by, $V_u = T_uE_x \subset T_uE$, where $\pi(u) = x$ and $\pi^{-1}(x) = E_x$ for $x \in M$.

Alternatively, the vertical subspace can be defined as the kernel of the push-forward of the projection map, $V_u = ker(T_u\pi)$, $u \in E$. Any arbitrary fiber bundle admits a connection. A special kind of Ehresmann connection is the principal connection.

Definition 5.5.2. (Principal connection) Let (P, M, G, π) be a smooth principal fiber bundle, where P is the total space, M the base space, F the fiber space and π the projection map. A principal connection on P is an assignment of a smoothly varying assingnment of a horizontal subspace H_q of the tangent space T_qP, $\forall q \in P$, such that,

(i) H_q is the complement (transverse) of the direct sum decomposition of the tangent space with respect to the fiber, $T_qP = H_q \oplus V_q$

(ii) H_q is invariant under left action of G on P, that is, if $\phi_g\colon P \to P$ is defined as $\phi_g(q)\colon q \mapsto \phi_g q$, then $(\phi_g)_*(H_q) = H_{\phi_g q}$, $\forall g \in G$.

$(\phi_g)_*$ is the canonical 'push-forward' map, $(\phi_g)_*\colon T_qP \to T_{\phi_g q}P$ along the fiber direction. The assignment of the horizontal subspace H_q is unique to the connection. A connection on a principal bundle is a right invariant distribution of the tangent bundle that is transverse to the fiber at each point. The dimension of the horizontal subspace H_u is the same as the dimension the tangent space T_xM by the fact, $T_q\pi(H_q) = T_{\pi(q)}M$, where $\pi(q) = x$.

Since the fiber group in the bundle is a Lie group, the tangent space to the fiber can be canonically identified with the tangent space at the identity, which is the Lie algebra $\mathfrak{g}$ of the group; i.e. $T_gG \cong \mathfrak{g}$. Given a connection Γ on a principal fiber bundle P, a Lie algebra valued 1-form ω can be defined on P. It may be noted that every Lie algebra element, $\xi \in \mathfrak{g}$ induces a infinitesimal generator vector field $\xi_P(q)$ on TP, $\forall q \in P$. Alternatively, a prinicipal connection can also be defined as folllows.

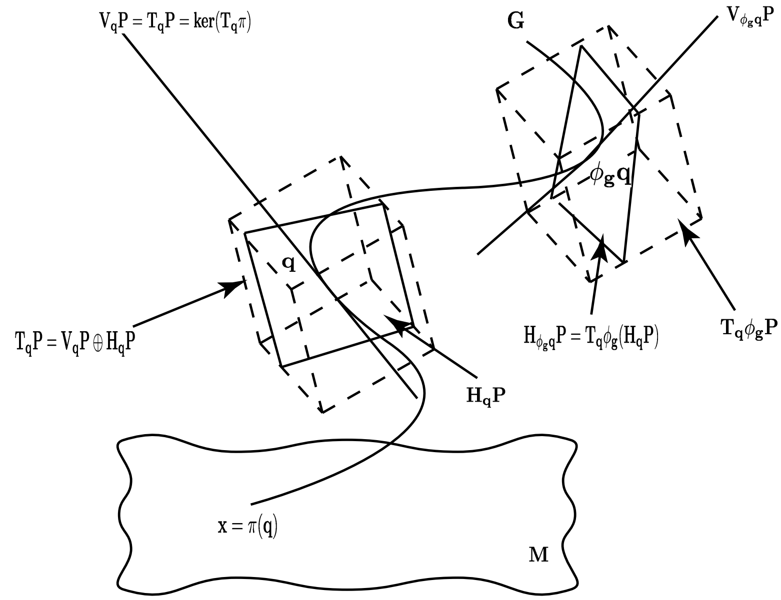

Figure 35: Principal connection

Definition 5.5.3. (Principal connection) A connection 1-form Γ_q on a principal bundle P is a Lie algebra-valued 1-form that satisfies, for each $q \in P$,

1. $\Gamma_q(\xi_P(q)) = \xi; \xi \in \mathfrak{g}$,

2. $\Gamma_{\phi_g(q)}(T_q\phi_g(v)) = Ad_g(\Gamma_q(v)); \forall v \in T_qP, \forall g \in G$.

The second condition implies that the connection form Γ is Ad-equivariant.

A curve $\tilde{c}(t)\colon [a,b] \to P$ on the bundle P is called a lift of a smooth curve $c(t)\colon [a,b] \to M$ in the base manifold M, if the projection map $\pi(\tilde{c}(t)) = c(t)$ for each t in $t \in [a,b]$. The curve $\tilde{c}(t)$ is a horizontal lift if the velocity vector $\dot{\tilde{c}}(t)$ lies in the horizontal subbundle HP, determined by the connection. For any piecewise C^∞ smooth curve $c(t)\colon [a,b] \to M$ in the base manifold M, such that $x_a = c(a)$ and $x_b = c(b)$, then at any point $q_a \in P_{x_a}$, there is a unique horizontal lift in the bundle, given by $\tilde{c}(t)\colon [a,b] \to P$, satisfying $\tilde{c}(a) = q_a$ [12]. For any piecewise smooth

$c(t)\colon [a,b] \to M$ curve in M, there exists a map $h_c\colon P_{x_a} \to P_{x_b}$ that maps q_a to $h_c(q_a)$ from the fibers E_{x_a} to E_{x_b}. This map is called parallel transport associated with the curve $c(t)$. The problem of constructing h_c for a vector field on M boils down to computing the integral curves of the horizontal lift of the vector field in the total space TQ, for an initial tangent vector. The map does not depend on the choice of parameterization of t for the curve $c(t)$ [22]. Associated with each connection form is a curvature form.

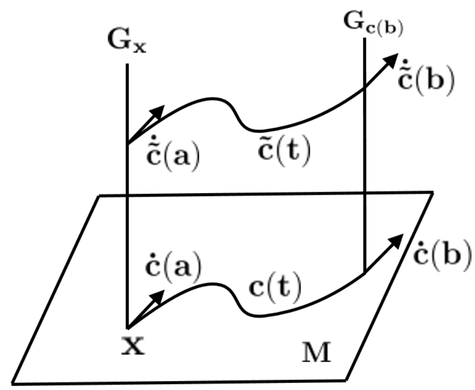

Figure 36: Parallel translation on principal fiber bundle

If $\Gamma\colon TP \to \mathfrak{g}$ be the connection 1-form, then the curvature of the connection is a 2-form given by the covariant exterior derivative of Γ,

$$D\Gamma(X,Y) = d\Gamma(X_h, Y_h) \tag{5.5.1}$$

where $X_h, Y_h \in HP$ for any two vector fields $X, Y \in \mathfrak{X}(P)$. The curvature form $D\Gamma\colon TP \times TP \to \mathfrak{g}$, for a connection form $\Gamma\colon TP \to \mathfrak{g}$, can be explicitly computed using the equation,

$$D\Gamma(X,Y) = d\Gamma(X,Y) - [\Gamma(X), \Gamma(Y)] \tag{5.5.2}$$

This equation is known as the Cartan's structure equation.

Let $c(t)\colon [a,b] \to M$ be a piecewise smooth closed curve in M passing through a reference point $x \in M$, such that $c(a) = x$ and $\pi^{-1}(x) = q$. Given a connection Γ in P, there exists a unique horizontal lift $\tilde{c}(t)\colon [a,b] \to P$ that generally maps q on to some other point $\tilde{c}(a) = p$ on the same fiber P_x (Fig.37). The points p and q are related by an equivalence $q \sim p$ for $p = gq$ where $g \in G$. The element g is called the geometric phase or holonomy of the curve $c(t)$. The holonomy group is defined as

$$\mathfrak{H}(q) = \{g \in G | q \sim gq\}. \tag{5.5.3}$$

If the parallel translation is restricted to contractible curves in M the subgroup that arises out of the holonomy group is called the restricted holonomy group, $\mathfrak{H}^0(q)$.

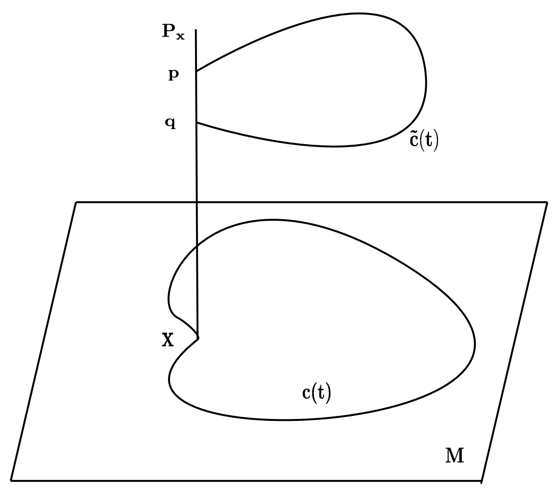

Figure 37: Holonomy on principal fiber bundle

5.6 Distributions And Frobenius Theorem

A k-dimensional distribution of a C^∞ manifold M is an assignment of a k-dimensional linear subspace $D_q \subset T_qM$ at each point $q \in M$. D_q is C^∞ with respect to q, if for some neighborhood $U \subset M$, there exists a set of vector fields $X^1, ..., X^k$ that span D_q for each $q \in U$. The vector fields $X^1, ..., X^k$ then form a basis of D_q. A submanifold $N \subset M$ is an integral submanifold if $T_qN = D_q$ for all $q \in M$. A distribution D is said to be integrable, if at each point of M there exists an integral manifold. If D is an integrable distribution, then for any two vector fields X and Y with $X_q, Y_q \in U$ for all q in some neighborhood $U \subset M$, the vector field $[X_q, Y_q] \in D_q$. Then distribution D is called involutive. An involutive distribution is integrable. An important result in the theory of integrability of submanifolds is the Frobenius theorem.

Theorem 5.6.1. (Frobenius theorem) A distribution D on a C^∞ manifold M is integrable, if and only if it is involutive.

5.7 Connection And Locomotion

The locomotion of certain classes of physical systems are driven by internal shape change. The mathematical representation of such systems can be done with a connection. The geometric aspects of the dynamics of mechanical systems with nonholonomic systems and symmetry have been dealt with in [3], [10]; among others. The utility of this approach is justified by the separation of dynamics of the shape and group variables in the reconstruction equation

$$g^{-1}\dot{g} = -A(r)\dot{r} + B(r)p. \tag{5.7.1}$$

The above equation is an expression of body fixed velocity $g^{-1}\dot{g}$ in terms of local connection form $A(r)$ and the generalized momentum p. If the body evolves on level set of zero initial momentum, the equation simplifies to

$$g^{-1}\dot{g} = -A(r)\dot{r}. \tag{5.7.2}$$

The momentum equation describes the evolution of the momentum as

$$\dot{p} = \dot{r}^T \alpha(r)\dot{r} + \dot{r}^T \beta r p + \dot{p}^T \gamma(r) p. \tag{5.7.3}$$

Some physical systems may be driven by conservation laws, some by constraints and the rest may be mix of both. In the kinematic case, the distribution (velocities that are annihilated by the constraint form) specified by the constraints provide a way to construct the connection. On the other hand, the presence of constraints may destroy the conservation laws in a system. The connection in a purely mechanical case is computed relative to a metric, the kinetic energy metric. There are three possible cases:

1. Kinematic connection: for systems governed by constraints
2. Mechanical connection: for systems governed by conservation laws
3. Nonholonomic connection: for systems governed by conervation laws and constraints

The kinematic and mechanical connections for two separate instances are worked out as illustrations in the present and subsequent chapter.

5.7.1 Principal kinematic connection

An example of a physical system that can be implemented by a kinematic connection is the kinematic car, a general abstraction of a car. The kinematic car has been worked out in [11], [10]. The position and orientation of the car is designated by the triplet (X, Y, θ) with respect to an inertial frame of reference. The steering angle and the angular rotation of the wheels is given by ϕ and ψ respectively. The configuration space of the system is $Q = SE(2) \times \mathbb{S}^1 \times \mathbb{S}^1$ or $Q = SE(2) \times \mathbb{T}^2$.

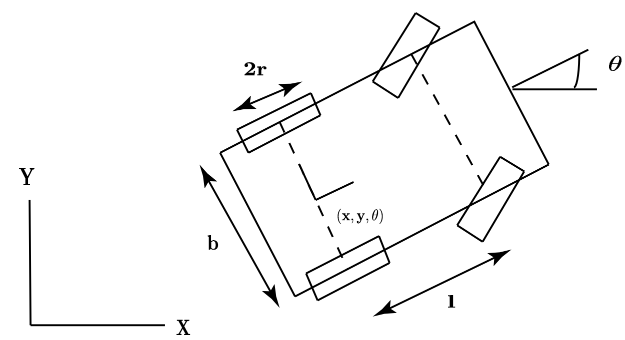

Figure 38: Kinematic car

The constraints that act on the car can be modeled as follows.

1. The rear cannot slip along the transverse to the longitudinal direction,

$$\dot{x}\sin\theta - \dot{y}\cos\theta = 0. \tag{5.7.4}$$

2. The front wheel does not slip in the direction transverse to the direction of rolling,

$$\dot{x}\sin(\theta + \phi) - \dot{y}\cos(\theta + \phi) - l\dot{\theta}\cos\phi = 0. \tag{5.7.5}$$

3. There is no slip of the rear wheels in the longitudinal direction,

$$\dot{x}\cos\theta + \dot{y}\sin\theta - r\dot{\psi} = 0. \tag{5.7.6}$$

Solving for $\dot{x}, \dot{y}$ and $\dot{\theta}$, the velocity at $q \in Q$ is given as

$$v_q = \begin{bmatrix} \dot{\psi} \\ \dot{\phi} \\ \dot{x} \\ \dot{y} \\ \dot{\theta} \end{bmatrix} = \begin{bmatrix} 0 \\ 0 \\ r\dot{\psi}\cos\theta \\ r\dot{\psi}\sin\theta \\ \frac{(r\dot{\psi})}{l}\tan\phi \end{bmatrix}. \tag{5.7.7}$$

The velocity v_q can be decomposed into two mutually orthogonal complements, the vertical verv_q along the fiber direction,

$$\mathrm{ver}v_q = \begin{bmatrix} 0 \\ 0 \\ \dot{x} - r\dot{\psi}\cos\theta \\ \dot{y} - r\dot{\psi}\sin\theta \\ \dot{\theta} - \frac{(r\dot{\psi})}{l}\tan\phi \end{bmatrix} \tag{5.7.8}$$

and the horizontal horv_q (in compliance with the constraints),

$$\mathrm{hor}v_q = \begin{bmatrix} 0 \\ 0 \\ r\dot{\psi}\cos\theta \\ r\dot{\psi}\sin\theta \\ \frac{(r\dot{\psi})}{l}\tan\phi \end{bmatrix}. \tag{5.7.9}$$

It may be recalled that for a given Lie algebra element $\xi(\xi_x, \xi_y, \xi_\theta)$ the infinitesimal generator vector field on $SE(2)$ at (x, y, θ) is $(\xi_x - y\xi_\theta, \xi_y + x\xi_\theta, \xi_\theta)$. The connection $\Gamma(q)$ maps the velocity v_q to verv_q or ξ. So, one can solve for ξ_x, ξ_y and ξ_θ in terms of the configuration variables.

$$\Gamma(v_q) = \begin{bmatrix} \dot{x} - (r\cos\theta + \frac{ry}{l}\tan\phi)\dot{\psi} + y\dot{\theta} \\ \dot{y} - (r\sin\theta - \frac{rx}{l}\tan\phi)\dot{\psi} - x\dot{\theta} \\ \dot{\theta} - \frac{r}{l}\dot{\psi}\tan\phi \end{bmatrix}. \tag{5.7.10}$$

The local connection form $A(r)$ can be recovered by recasting the right hand side of the above equation in line with the reconstruction equation $Ad_g(g^{-1}\dot{g} + A(r)\dot{r})$. The local connection form works out to

$$A(\psi, \phi) = \begin{bmatrix} -rd\psi \\ 0 \\ -\frac{r}{l}\tan\phi d\phi \end{bmatrix}. \tag{5.7.11}$$

CHAPTER 6: CHAOS IN PRINCIPAL FIBER BUNDLE

Dynamical systems that have principal fiber bundles as configuration spaces are of interest from the mathematical standpoint. The differential equations of motion can be written explicitly as input-output systems, where the input variables can be decoupled from output variables. The reduction technique for systems with symmetry, as well as for systems with nonholonomic constraints has been enunciated in previous chapter. The behavior of the system, characterized by the group variables (output), under chaotic actuation of the shape variables (input) is of special concern. The connection of the system, as modeled either by the energy metric or the constraints or both, is essentially a map from the shape manifold to the group manifold. Whether the connection preserves the topological property of a chaotic vector field in the shape space when mapped onto the group space, is relevant to the investigation of chaos in Riemannian manifolds that have product structure. Relatedly, a system with symmetry and modeled by principal connection is implemented using the reduction techniques on principal fiber bundle in this document. The shape variables are excited by a chaotic control input. The motion of the body, given by the group variables, is investigated for presence of chaos.

The mass-beanie system that will be introduced later in the chapter is used to illustrate the result. The beanie is actuated by the Lorentz vector field and the evolution of the beanie is along trajectories on the strange attractor. The configuration space of the system is $SE(2) \times SE(2)$. The Lie group $SE(2)$ is a Riemannian manifold that can be equipped with a smoothly varying inner product at each point. In the next section, we recall some of the properties the Lie group $SE(2)$ and construct a Riemannian norm in the manifold [8].

6.1 Special Euclidean Group $SE(2)$

The special Euclidean group is the group of all translations and rotations on the Euclidean group $\mathbb{R}^2$. It is a semidirect product of the Lie groups the group of planar translations $\mathbb{R}^2$ and the group of rotations in a plane $SO(2)$.

6.1.1 The Lie group $SE(2)$

A member of $SE(2)$ is represented by a pair $g = (R_\theta, x)$, where $R_\theta \in SO(2)$ and $x \in \mathbb{R}^2$. The elements of the group $SE(2)$ is in one to one correspondence with the set of all transformation matrices of the form

$$\hat{g} = \begin{pmatrix} R_\theta & x \\ 0 & 1 \end{pmatrix}. \tag{6.1.1}$$

As a topological space $SE(2)$ is homeomorphic to the product group $\mathbb{R}^2 \times \mathbb{S}(1)$. The elements of $SE(2)$ act on each other by translation which is the group multiplication. In terms of matrix multiplication, this can be written as

$$\hat{g}_1 \cdot \hat{g}_2 = (R_\theta, x) \cdot (R_\phi, y) = (R_{\theta+\phi}, R_\theta y + x). \tag{6.1.2}$$

The inverse group operation is given by,

$$(R_\theta, x)^{-1} = (R_{-\theta}, -R_{-\theta} x). \tag{6.1.3}$$

6.1.2 The Lie algebra $\mathfrak{se}(2)$

The Lie algebra of the $SE(2)$ is the linear vector subspace at the identity of the group that is closed under matrix addition and scalar multiplication and is equipped with a matrix commutator bracket $[\cdot,\cdot]$. The Lie algebra is denoted by $\mathfrak{se}(2)$. The elements of the Lie algebra can be viewed as infinitesimal planar translations and rotations. The representation of the Lie algebra is a vector $\xi = (\xi_x, \xi_y, \xi_\theta) \in \mathbb{R}^3$. The Lie algebra elements ξ share a one to one correspondence with the set all 3×3 matrices of the form

$$\hat{\xi} = \begin{pmatrix} 0 & -\xi_\theta & \xi_x \\ \xi_\theta & 0 & \xi_y \\ 0 & 0 & 0 \end{pmatrix}. \tag{6.1.4}$$

The Lie bracket on $\mathfrak{se}(2)$ is the matrix commutator defined as

$$[\hat{\xi}, \hat{\eta}] = \hat{\xi}\hat{\eta} - \hat{\eta}\hat{\xi}. \tag{6.1.5}$$

The linear vector space dual to $\mathfrak{se}(2)$ is the dual of the Lie algebra and is denoted as $\mathfrak{se}(2)^*$. The element wise representation of $\mathfrak{se}(2)^*$ is given as $\pi = (\pi_x, \pi_y, \pi_\theta) \in \mathbb{R}^3$. The group $SE(2)$ being a Riemannian manifold, is equipped with a smoothly varying inner product that is defined in terms of the Euclidean inner product on $\mathbb{R}^3$. The elements of the Lie agebra and the dual space are paired naturally by the inner product by

$$(\pi, \xi) = \pi^T \xi = \xi_\theta \pi_\theta + \begin{bmatrix} \pi_x \\ \pi_y \end{bmatrix} \begin{bmatrix} \xi_x & \xi_y \end{bmatrix} \tag{6.1.6}$$

for $\xi \in \mathfrak{se}(2)$ and $\pi \in \mathfrak{se}(2)^*$.

6.1.3 Choice of norm on $SE(2)$

For any fixed parameter $m > 0$, a suitable left-invariant norm can be defined on $\mathfrak{se}(2)$ by

$$||\xi||^2_{\mathfrak{se}(2)} := m\xi_\theta^2 + \begin{bmatrix} \xi_x \\ \xi_y \end{bmatrix} \begin{bmatrix} \xi_x & \xi_y \end{bmatrix} \tag{6.1.7}$$

for $\xi \in \mathfrak{se}(2)$ [8]. A left invariant norm can be constructed on the tangent space of the group by left translation of the Lie algebra vectors, such that

$$||v_g||^2_{SE(2)} = ||T_g L_{g^{-1}} v_g||^2_{\mathfrak{se}(2)} \tag{6.1.8}$$

for all $g \in SE(2)$ and $v_g \in T_g SE(2)$. The standard representation of an element $g \in SE(2)$ is given as

$$g = \begin{bmatrix} \cos\theta & -\sin\theta & x \\ \sin\theta & \cos\theta & y \\ 0 & 0 & 1 \end{bmatrix} \tag{6.1.9}$$

and

$$v_g = \begin{bmatrix} \dot{x} & \dot{y} & \dot{\theta} \end{bmatrix} \tag{6.1.10}$$

for $v_g \in T_g SE(2)$. The norm on $SE(2)$ can be computed by plugging in v_g in to equation (8),

$$||v_g||^2_{SE(2)} = m\dot{\theta}^2 + \begin{bmatrix} \dot{x} \\ \dot{y} \end{bmatrix} \begin{bmatrix} \dot{x} & \dot{y} \end{bmatrix}. \tag{6.1.11}$$

The left invariant property of the norm under left translation of the group $SE(2)$ can be shown as follows,

$$||(T_g L_h)v_g||^2_{SE(2)} = ||(T_g L_{hg^{-1}})(T_g L_h)v_g||^2_{\mathfrak{se}(2)} = ||(T_g L_{g^{-1}})v_g||^2_{\mathfrak{se}(2)} = ||v_g||^2_{SE(2)}. \tag{6.1.12}$$

6.2 Ellipse With A Beanie

An ellipse with a beanie mounted on it is an example of a dynamical system that generates locomotion by internal shape change. The beanie is kinematically coupled with the ellipse at the base. In the absence of external forces and moments, the system is governed by conservation laws; conservation of linear and angular momentum. The dynamics of the beanie causes the motion of the ellipse in a manner, that the system evolves on level sets of initial momentum. A dynamical system that is driven by internal shape change can be reduced by exploiting the symmetries of the system. The theory of such reduction is expounded in [3]. As the motion of the system is restriced to a plane, the position and orientation of the ellipse is sufficient to identify the system in configuration space. The position and orientation of center of mass of the ellipse O is x,y and θ, expressed relative to an inertial frame (X-Y), while the position and orientation of center of mass A of the beanie is ξ, η and ϕ, referenced with respect to body fixed axes (ξ-η), located at the intersection of the principal axes of the ellipse.

The configuration space of the system is a principal fiber bundle: $Q = SE(2) \times SE(2)$. The longitudinal and lateral translational inertia of the ellipse are denoted by M_{long} and M_{lat} respectively and the beanie is of mass m. The rotational intertia

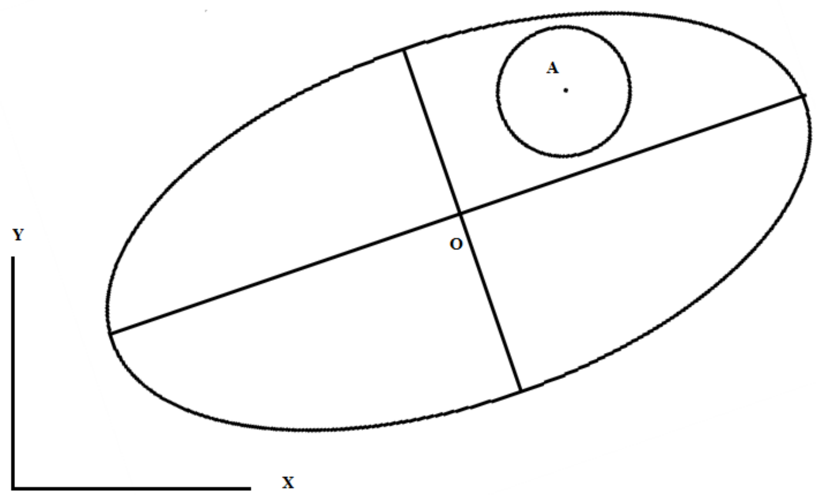

Figure 39: Ellipse with a beanie

and angular displacement about the axis of rotation of the ellipse and the beanie are b, θ, c, ϕ, correspondingly. The position of the ellipse and beanie is given by

$$X_{ellipse} = [x, y] \tag{6.2.1a}$$

$$X_{beanie} = [x + \xi \cos\theta - \eta \sin\theta, y + \xi \sin\theta + \eta \cos\theta]. \tag{6.2.1b}$$

The Lagrangian of the system L, which is the difference of kinetic and potential energy of the system is

$$L = \frac{1}{2}M_{long}[\dot{x}\cos\theta + \dot{y}\sin\theta]^2 + \frac{1}{2}M_{lat}[-\dot{x}\sin\theta + \dot{y}\cos\theta]^2 + \frac{1}{2}m([\dot{x} - \dot{\eta}\sin\theta - \eta\dot{\theta}\cos\theta - \xi\dot{\theta}\sin\theta + \dot{\xi}\cos\theta]^2 + [\dot{y} + \dot{\eta}\cos\theta - \eta\dot{\theta}\sin\theta + \xi\dot{\theta}\cos\theta + \dot{\xi}\sin\theta]^2) + \frac{1}{2}b\dot{\theta}^2 + \frac{1}{2}c[\dot{\theta} + \dot{\phi}]^2. \tag{6.2.2}$$

The group action of $g \in G$ on the tangent bundle TQ leaves the Lagrangian $L\colon TQ \to \mathbb{R}$ invariant. The left invariant metric defined in the earlier section is the one associated with the kinetic energy metric of our system. As the evolution of the system is solely governed by symmetries, the connection on the principal tangent bundle TQ is a mechanical connection. The principal bundle, in this case, comprises the base manifold $M = Q/G$ populated by the fiber group G. The mechanical connection Γ can be computed from the fact that the horizontal subspace of the tangent space at a point $q \in Q$ is the space obtained by the orthogonal complement of the tangent space of the fiber (group orbit), relative to the kinetic energy metric. In order to derive an expression for the momentum map $\mathbb{J}$, the fiber derivative map $\mathbb{FL}$ needs to be defined. The fiber derivative $\mathbb{FL}\colon TQ \to T^*Q$ is defined in coordinate-free manner as the derivative of the Langrangian along the fiber direction by

$$\langle \mathbb{FL}(q, v_q), w_q \rangle = \frac{dL}{dt}(q, v_q + tw_q)|_{t=0} \tag{6.2.3}$$

for $q \in Q$ and $v_q, w_q \in T_qQ$. For finite dimensional systems, in local coordinates, the fiber derivative has the expression $\mathbb{FL}(q, \dot{q}) = \frac{\partial L}{\partial \dot{q}}$, for $q \in Q$. The momentum map

$\mathbb{J} \colon TQ \to \mathfrak{g}^*$ is expressed as

$$\langle \mathbb{J}(q, \dot{q}), \xi \rangle = \langle \mathbb{FL}(q, \dot{q}), \xi_Q(q) \rangle. \tag{6.2.4}$$

The locked inertia tensor $\mathbb{I}$ can then be computed using the expression

$$\langle \mathbb{I}(q, \dot{q}, \xi, \eta) \rangle = \langle \langle \xi_Q(q), \eta_Q(q) \rangle \rangle \tag{6.2.5}$$

where $\xi_Q(q)$ and $\eta_Q(q)$ represent the infinitesimal generator vector fields corresponding to Lie algebra elements ξ and η and the double angular brace indicates the kinetic energy metric. The mechanical connection $\Gamma \colon TQ \to \mathfrak{g}^*$ is an equivariant, 'dual of the Lie algebra valued' map and can be computed explicity from the equation

$$\Gamma(q, (\dot{q})) = \mathbb{I}^{-1}\mathbb{J}. \tag{6.2.6}$$

The mechanical connection enables one to express the dynamics of the system in terms of its internal shape variables. This equation describes the evolution of the group variable g and is known as reconstruction equation,

$$\Gamma = Ad_g(g^{-1}\dot{g} + A(r)\dot{r}). \tag{6.2.7}$$

The term $A(r)$ is the local locked inertia tensor and is designated as $A(r) \colon TM \to \mathfrak{g}^*$.

6.2.1 Chaos in principal fiber bundle

The local connection form $A(r)$ can be viewed as a map of the shape vector fields in TM to $\mathfrak{g}$, which is naturally identified with the tangent space of the fiber group. The velocities of the shape variables represent control inputs to the physical system; the group velocities being the output as modeled by the mechanical connection. The control vector fields in the shape space could be that of standard fixed points, like attractors, repellers, saddle points or centers. The evolution of the group variables in such cases present an interesting case study. As an example, the solution for the group variables are plotted when the ordinary differential equations for the control input happen to be a center. The shape space vector fields are given as

$$\dot{\xi} = -\sin(t) \tag{6.2.8a}$$

$$\dot{\eta} = \frac{1}{\sqrt{2}}\cos(t) \tag{6.2.8b}$$

$$\dot{\eta} = \frac{1}{\sqrt{2}}\cos(t). \tag{6.2.8c}$$

The integral curve of the solution indicate a monotonically increasing θ, thus eliminating the presence of a center in the group space (Fig.40).

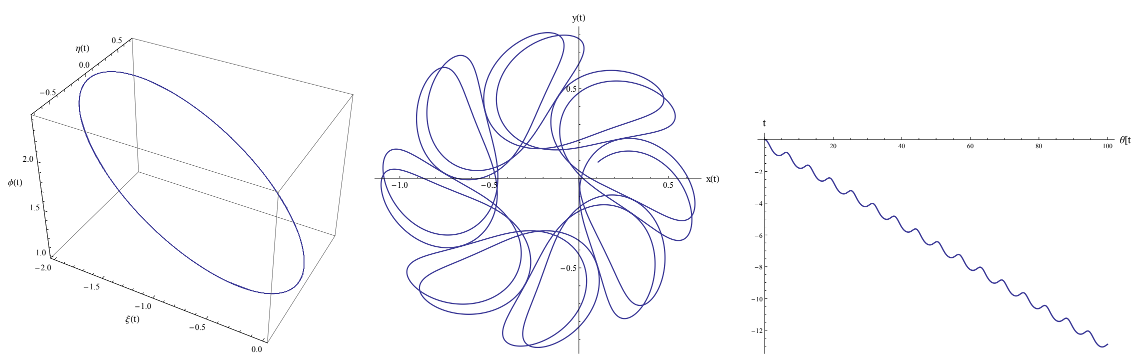

(a) Plot of shape variables (b) Plot of x[t] and y[t] in group space (c) Plot of θ in group space

Figure 40: Plot of group variables for center control vector field

The control vector fields on shape manifold, for a given mechanical connection, determine the evolution of the group variables of the physical system. The scope of the present research involves studying the motion of the body along the fiber when the vector field in the shape space is chaotic. The connection of the system determines the motion of the body for a given control input. In the 'ellipse with a beanie' example, the Lorenz equations describe the trajectory of the beanie. The plots of the group group variables is indicative of non-chaotic nature of the system dynamics.

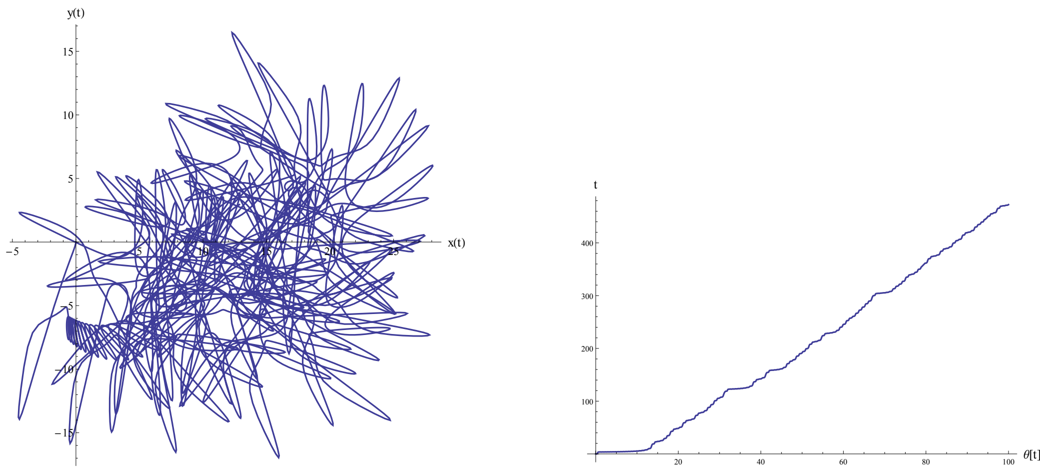

(a) Trajectory of ellipse in $x(t)$-$y(t)$ plane (b) θ vs t for the ellipse

Figure 41: Evolution of the ellipse under chaotic shape actuation

It is worth noting that the variable θ is identified with group $\mathbb{R}$ and not with the quotient group $\mathbb{R}/2\pi$. The group $\mathbb{S}^1$ can be shown to be homeomorphic to the real number line $\mathbb{R}$ by 'one point compactification'. The representation of θ by $\mathbb{R}$ is done to make the distinction between rotations that are integral multiples of 2π of each other.

6.2.2 Lyapunov exponents on $SE(2)$

The equations of motion of the ellipse can be expressed in terms of body fixed coordinates solely by internal shape variables. The aforementioned reduction technique is employed to arrive at the reduced equations of motion. The Lyapunov exponents are computed by solving a set of coupled differential equations, consisting of the vector field and its differential. The technique has been outlined in chapter 2 of the document. The fact that the steady state values of the three Lyapunov exponents are positive, indicate a departure from chaos (Fig.42). The evolution of the configuration space variables are plotted by solving the reduced differential equations of motion in terms of shape variables.

$$\dot{x} = \frac{10\left(\xi^2+4\right)(\eta-\xi)}{2\left(2\eta^2+6\right)+3\xi^2} + \frac{\eta\xi(\xi(28-\phi)-\eta)}{2\left(2\eta^2+6\right)+3\xi^2} + \frac{2\eta\left(\eta\xi-\frac{8\phi}{3}\right)}{2\left(2\eta^2+6\right)+3\xi^2} \tag{6.2.9a}$$

$$\dot{y} = \frac{20\eta\xi(\eta-\xi)}{2\left(2\eta^2+6\right)+3\xi^2} + \frac{\left(2\eta^2+6\right)(\xi(28-\phi)-\eta)}{2\left(2\eta^2+6\right)+3\xi^2} - \frac{3\xi\left(\eta\xi-\frac{8\phi}{3}\right)}{2\left(2\eta^2+6\right)+3\xi^2} \tag{6.2.9b}$$

$$\dot{\theta} = -\frac{40\eta(\eta-\xi)}{2\left(2\eta^2+6\right)+3\xi^2} + \frac{3\xi(\xi(28-\phi)-\eta)}{2\left(2\eta^2+6\right)+3\xi^2} + \frac{6\left(\eta\xi-\frac{8\phi}{3}\right)}{2\left(2\eta^2+6\right)+3\xi^2} \tag{6.2.9c}$$

The above equations are devoid of shape velocity terms $\dot{\xi}, \dot{\eta}$ and $\dot{\phi}$ as they have been substitued in the by the control vector fields which are given below:

$$\dot{\xi} = 10\,(\eta-\xi) \tag{6.2.10a}$$

$$\dot{\eta} = \xi\,(28-\phi)-\eta \tag{6.2.10b}$$

$$\dot{\phi} = \xi\eta - \frac{8}{3}\phi \tag{6.2.10c}$$

Of the three Lyapunov exponents of the Lorenz system on $\mathbb{R}^3$, one equals zero and the absolute value of the positive exponent is smaller than the absolute value of the negative exponent. In case of Hamiltonian systems, the nonzero Lyapunov exponents are equal in magnitude and opposite in sign. If all three Lyapunov exponents end up being positive, the system is non-dissipative in nature. It suggests that the configuration space corresponding to all three directions along which the exponents are measured, are stretching at exponential rates.

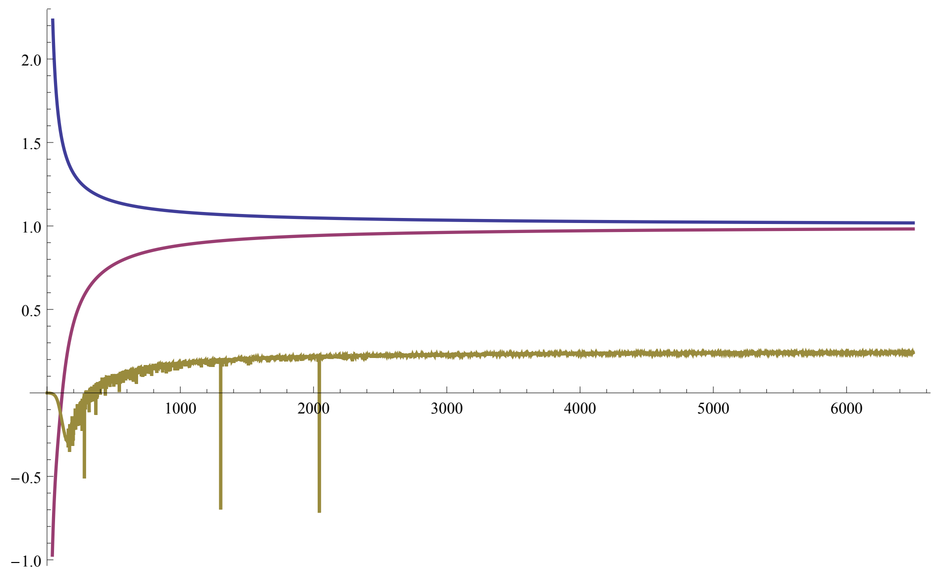

Figure 42: Lyapunov spectrum

CHAPTER 7: CONCLUSION AND FUTURE WORK

7.1 Chaos In Riemannian Geometry

Dynamical systems that exhibit chaos differ from other nonlinear systems in terms of their sensitivity to initial conditions, transitivity and topological mixing. The 'stretching and folding' of the phase space uniquely characterizes a chaotic system. The study of chaos with reference to surface geometry is one of the objectives of this thesis. The characterization of chaos may be influenced by the topology that one defines on the topological space. As an example, a discrete topological space is a topological space that is equipped with a metric

$$d(x,y) = \begin{cases} 1, & \text{if } x\text{=y} \\ 0, & \text{if } x \neq \text{y}. \end{cases}$$

The Lyapunov exponents for a dynamical system, in discrete space, can either be 0 or 1. The canonical notions of manifolds on the phase space, such as attractor, repeller etc. on such a space are different from that of $\mathbb{R}^3$. In chapter 4 of the document, the Lorenz equations have been examined for chaos under a diffeomorphic map (stereographic projection) on $\mathbb{S}^3$. The study can be extended to other Riemannian manifolds, like $\mathbb{T}^3$. A comparative examination of different spaces, equipped with different metrics, can be carried out with reference to compactness and non-compactness and abelianness and nonabelianness of the spaces. The study of chaos could include other instances of non-Euclidean geometry, like hyperbolic geometry. Among the models of hyperbolic geometry, the hyperboloid model has been studied with reference to sensitivity to initial conditions for the Lorenz system. The solution of the Lorenz equations is projected onto the forward sheet of a three dimensional hyperboloid, embedded in $\mathbb{R}^4$ and given by the equation

$$x^2 - y^2 - z^2 - w^2 = 1. \tag{7.1.1}$$

The coordinate w was computed in terms of x, y, z, which are the solutions of the Lorenz system. Using the distance metric for the hyperboloid model, the maximum Lyapunov exponent was computed to be 2×10^3.

7.2 Systems Modeled By Connection

Dynamical systems that generate locomotion by internal shape change are modeled by connection. A system that is governed solely by symmetry (conservation laws) gives rise to a mechanical connection. If the configuration space happens to be a Lie group, by exploiting the symmetry of the system, the equations of motion can be expressed in terms of shape variables. The nature of evolution of the group variables for chaotic control input in the shape space is an area of interest. As an example, the motion of an ellipse-with-a-beanie in an ideal fluid has been examined for chaotic actuation of the shape variables. The investigation of behavior of group variables under the connection map could include other connection forms. A connection derived from the constraint equations is kinematic. Nonholonomic connection is a constraint that is derived from the distribution specified by the constraints as well as from symmetry consideration. The effect of chaotic actuation of the shape variables on the evolution of group variables, for such systems is part of wider problem of investigating chaos in different configuartion spaces.

7.3 Left Invariant Vector Fields And Lie Algebra

A left invariant vector field on a Lie group can be generated by the push-forward of a Lie algebra element at the identity by the group action. If the vector field defined by the Lie algebra elements of a three dimensional Lie algebra (with respect to a three dimensional basis) is the Lorenz vector field, the nature of evolution of the group velocities under the tangent lifted map, is an area of interest. This problem amounts to solving for the flow of a time-varying six-dimensional set of ordinary differential equations. In physical terms, this is analogous to examining for chaos, the motion of a body in an inertial frame of reference, when the measured velocities in the body frame of reference happen to be chaotic. The inverse of problem could as well be posed as, investigating for chaos in the body fixed reference frame, when the motion of the body with respect to an inertial reference frame happen to be chaotic. The pullback of the group velocities at the Lie algebra should be studied for chaos, in such case. The suggestive Lie groups could be $\mathbb{R}^3$, $SE(2)$ or $SO(3)$. It is worthwhile to bear in mind that push-forward by the group action for $\mathbb{R}^3$ is the identity map.

REFERENCES

[1] J. Banks, J. Brooks, G. Cairns, G. Davis, and P. Stacey. On Devaney's definition of chaos. *The American Mathematical Monthly*, 99(4):332–334, 1992.

[2] G. Benettin, L. Galgani, A. Giorgilli, and J. Strelcyn. Lyapunov characteristic exponents for smooth dynamical systems and for Hamiltonian systems: A method for computing all of them. Part 2: Numerical application. *Mecanicca*, 15:21–30, 1980.

[3] A. Bloch, P. Krishnaprasad, J. Marsden, and R. Murray. Nonholonomic mechanical systems with symmetry. *Archive of Rational Mechanics*, 136:21–99, 1996.

[4] R. Devaney. *An Introduction to Chaotic Dynamical Systems*. Addison-Wesley Publishing Company, Inc., 1989.

[5] K. J. Falconer. *The Geometry of Fractal Sets*. Cambridge University Press, 1986.

[6] T. Gamelin and R. Green. *Introduction to Topology*. Dover, 1999.

[7] K. Gillow. *Codimension-two free boundary problems*. PhD thesis, Oxford, 1998.

[8] D. Holm, L. Noakes, and J. Vankerschaver. Relative geodesics in the special Euclidean group. *Proceedings of the Royal Society*, A 469:20130297, 2013.

[9] D. Holm, T. Schmah, and C. Stoica. *Geometric Mechanics and Symmetry*. Oxford University Press, 2009.

[10] S. Kelly. *The Mechanics and Robotic Locomotion with Application to Aquatic Vehicles*. PhD thesis, California Institute of Technology, 1998.

[11] S. Kelly and R. Murray. Geometric phases and robotic locomotion. *J. Robotic Systems*, 12(6):417–431, 1995.

[12] K. Kobayashi and K. Nomizu. *Foundations of Differential Geometry, Vol-1*. Wiley Classics Library, 1996.

[13] K. Kuznetsov. *Elements of Applied Bifurcation Theory*. Springer, 2004.

[14] H. Lamb. *Hydrodnamics*. Dover Publishing Company, 1993.

[15] J. Lee. *Riemannian Manifolds: An Introduction to Curvature*. Springer, 1997.

[16] J. Lee. *Introduction to Smooth Manifolds*. Springer, 2003.

[17] F. Lekien and S. Ross. The computation of finite-time Lyapunov exponents on unstructured meshes and for non-Euclidean manifolds. *Chaos*, 20:017505, 2010.

[18] J. Marsden and T. Ratiu. Reduction of Poisson manifolds. *Letters in Mathematical Physics*, 11:161–169, 1986.

[19] J. Marsden and T. Ratiu. *Introduction to Mechanics and Symmetry*. Springer, 1999.

[20] J. Marsden and A. Weinstein. Reduction of symplectic manifold with symmetry. *Reports on Mathematical Physics*, 5:121–130, 1974.

[21] L. Milne-Thomson. *Theoretical Hydrodynamics*. Dover, 2011.

[22] S. Morita. *Geometry of Differential Forms*. American Mathematical Society, 1998.

[23] D. E. Neuenschwander. *Emmy Noether's Wonderful Theorem*. Johns Hopkins University Press, 2010.

[24] V. Oseledec. A multiplicative ergodic theorem: Lyapunov characteristic numbers for dynamical systems. *Trans. Moscow Mathematical Society*, 19:197–231, 1968.

[25] T. Parker and L. Chua. *Practical Numerical Algorithms for Chaotic Systems*. New York: Springer-Verlag, 1989.

[26] L. Perko. *Differential Equations and Dynamical Systems*. Springer, 2001.

[27] M. Sandri. Numerical calculations of Lyapunov exponents. *The Mathematica Journal*, 6(3):78–84, 1996.

[28] M. Sano and Y. Sawada. Measurement of the Lyapunov spectrum from a chaotic time series. *Physical Letter Review*, 55:1082, 1985.

[29] S. Schecter and M. Singer. A class of vector fields on $\mathbf{S}^2$ that are topologically equivalent to polynomial vector fields. *Journal of Differential Equations*, 57:406–435, 1985.

[30] C. Sparrow. *The Lorenz Equations: Bifurcations, Chaos, and Strange Attractors*. Springer Verlag, 1982.

[31] S. H. Strogatz. *Nonlinear Dynamics and Chaos*. Westview Press, 2000.

[32] S. Wiggins. *Introduction to Nonlinear Dynamical Systems and Chaos*. Springer, 2003.

[33] A. Wolf, J. Swift, H. Swinney, and J. Vastano. Determining Lyapunov exponents from a time series. *Physica D*, 16:285–317, 1985.